International Journal of Refractory Metals and Hard Materials

# Effect of chromium and carbon contents on the sintering of WC-Fe-Ni-Co-Cr multicomponent alloys

--Manuscript Draft--

| | |
|---|---|
| **Manuscript Number:** | IJRMHM-D-20-00205R1 |
| **Article Type:** | Research Paper |
| **Keywords:** | Tungsten carbide, Fe-Ni-Co-Cr binder, sintering, thermal analysis, precipitation of Cr carbides |
| **Corresponding Author:** | Jose M. Sanchez<br>CEIT-IK4<br>San Sebastian, Guipuzcoa SPAIN |
| **First Author:** | T. Soria-Biurrun, Degree in Chemical Science |
| **Order of Authors:** | T. Soria-Biurrun, Degree in Chemical Science |
| | L. Lozada-Cabezas, Ph.D. Chemistry |
| | F. Ibarreta-Lopez, Degree in Chemical Science |
| | R. Martinez-Pampliega, Industrial Engineer |
| | Jose M. Sanchez |
| **Abstract:** | WC-Fe-Ni-Co-Cr cemented carbides have been obtained by liquid phase sintering from WC-Fe-Ni-Co-Cr 3 C 2 powder mixtures. Taking the 40wt.%Fe-40wt.%Ni-20wt.%Co alloy as a reference, new binder phases has been prepared by introducing controlled amounts of Cr and C, via Cr 3 C 2 and C black powders respectively. As described for WC-Co-Cr materials, Cr additions are also observed to reduce the eutectic temperatures of WC-Fe-Ni-Co system. First liquids detected on heating exhibit wide temperature melting ranges, which become narrower and are displaced to higher temperatures on repeated heating and cooling cycles. Apart from the decarburization associated to the carbothermal reduction of powder oxides, this phenomenon could be also related to the homogenization of the chemical composition of these multicomponent binder phases, which is faster as C content decreases. Correlation between experimental melting and solidification temperature ranges and those predicted by Thermocalc® is better as Cr content increases. Experimental C windows, defined in this work by the absence of free C or h phases, are located at C contents higher than Thermocalc® estimations. Although the 40wt.%Fe-40wt.%Ni-20wt.%Co alloy is austenitc, BCC phases are partially stabilized at low C and high Cr contents. Although these compositions are free from h phases or free C, a precipitation of Cr-rich carbides is found at the WC-metal interface. These precipitates are not observed in the alloy with 0.75 wt.% Cr (i.e. 5 wt.% of the nominal metal content) and 5.39 wt.%C. This C content is 0.17 wt.% higher than that predicted for precipitation of M 7 C 3 . |
| **Response to Reviewers:** | Ref: IJRMHM-D-20-00205<br>Title: Effect of Cr anc C contents on the sintering of WC-Fe-Ni-Co-Cr multicomponent alloys<br><br>Journal: International Journal of Refractory Metals and Hard Materials<br><br>We have included some equations and SEM images in the respond to reviewers. Complete information appears before the pdf of the revised manuscript. Please, find equations and images in that pdf format. In this box, neither images nor equations are allowed.<br><br>Answers to Reviewer # 1 comments:<br><br>1-Authors should give details about the powders used, especially the particle size. A micrograph of a powder compact would be useful to appreciate the heterogeneity in the powder mixtures, which is the reason given by the authors for the broad temperature range of liquid formation. |

Answer: We definitely agree with the referee's comment. In the new version, we have included a new Table 1 at the beginning of section 2 with the particle size of starting powders. We have also included a new Fig. 2 corresponding to a green compact of composition C4 (medium C content) (see new Table 2). A paragraph has been included in Section 3.1(a) of the revised version that provides the requested information about the scale of microstructural segregation in the green compacts.

2.The authors state that sintering starts at higher temperatures for the W-rich alloys. But from the dilatometric plots, it appears that sintering (apparently solid state sintering) starts at a lower temperature for these alloys. This is indeed a classical result of solid state sintering of WC-Co alloys which has been observed by several authors, and is probably related to a better solid state spreading of the binder due to a lower interface energy in W-rich alloys (see e.g. A. Petersson, Int. J. Refractory Metals & Hard Materials 22(4-5), 2004, 211-217). The authors probably mean that the liquid phase sintering peak is delayed to higher temperatures for the W-rich alloys but this should be clarified.

Answer: Yes. Our intention was to describe melting phenomena and not shrinkage in solid state. Again, we thank the referee for the precise comment. We have modified the text in order to include it along with two additional references [22 and 23 in the new version]. The new text is included at the beginning of Section 3.1. (a), in the part explaining Fig. 1.

3.The authors should be careful when relating the area of endothermic peaks to the amount of liquid, since the composition may influence the enthalpy of melting. And from figure 1 c), I would not say that area of the endothermic peak on cooling is 100% higher for the C2 alloys, since the peak for C1 alloy is broader. Did they make a measurement or is this a rough estimate?

Answer: After the reviewer's comment, we have revised the calculation of DSC peak areas and found that the melting range we considered for Alloy C1 was only from 1300ºC to 1380ºC. We agree that there is some liquid above 1261ºC. Considering this, the area under the DSC peak of Alloy C1 (High C) for the first heating event is still 30% lower than that calculated for alloy C2 (Low C). We have also corrected the areas corresponding to exothermic peaks, which are also higher for Alloy C2 than for Alloy C1, but only by 20%.
The theory behind the calculation of the amount of liquid is explained in the pdf version of this "Respond to Reviewers", found before the pdf of the revised manuscript.

We have also revised the bibliography to the best of our knowledge and have not found information regarding the enthalpies of melting for Fe-Ni-Co-Cr-W alloys. Therefore, the correlation between areas of DSC peaks and actual liquid contents is only qualitative.
The method for calculating DSC peak areas and this final comment have been included in the revised text.

4.More important, the authors explain the effect of C content on the temperature of liquid formation by homogenization of the metallic binder composition. They argue that a Fe-rich liquid would form at lower temperature for C-rich alloys. But I do not understand the reason why this Fe-rich liquid would form rather in C-rich rather than in W-rich alloys. In addition, for a binder with uniform composition, the solidus temperature increases when decreasing the C content, as predicted by the phase diagrams (see Fig. 6) and this must have a first-order effect on the temperature of liquid formation, before incriminating a metallic composition gradient in the binder. Finally, the DSC plots after several runs show the same position for the peaks for alloys C1 and C2 on heating and on cooling, which suggests a decarburization of the alloys and a liquid formation which could correspond to the eutectic liquid on the W-rich side of the 2-phase domain for both compositions (see Fig. 6).This decarburization is

often an issue with the small samples used in DSC (1 mm3 here) for long or repeated thermal cycles. This discussion of the C content effect on the temperature of liquid formation should be rewritten by taking these remarks into consideration.

Answer: Of course, we agree with the referee's comment about the displacement of melting onset to higher temperatures as C activity decreases. This is a well-known effect in cemented carbides and, as the referee points out, is well reflected in our Thermocalc ® calculations.

We also agree on considering decarburization effects, although it is impossible to measure carbon contents in DSC samples owing to their small size. Repeated DSC experiments were carried out without opening the furnace chamber and always protected with pure Argon atmosphere (nominal oxygen and water contents in this gas are 2 ppm and 3 ppm respectively). Of course, the procedure includes leak testing and 3 purges of the calorimeter chamber to remove all residual air (the whole process takes 1. 5 hours). Main decarburization should be expected for the first DSC heating cycle due to carbothermal reduction of oxides present in the powder mixtures. In repeated DSC experiments, the samples have already a high degree of sintering. Therefore, the specimen surface area is considerably reduced and decarburization kinetics should be slower.

Anyhow, although samples can be decarburized during repeated DSC experiments, melting and solidification temperature intervals observed experimentally are very different from those calculated by Thermocalc ® with TCFE10 database. The isopleth of new Fig. 2; including both compositions C1 and C2, shows that the melting range of alloys near the upper C side of the 2 phase domain has a maximum value of 69ºC (far from the 122ºC measured experimentally for Alloy C1). On the lower C side, the melting range corresponding with no presence of M6C is only 9ºC. Again, far from the 51ºC measured experimentally for Alloy C2.
In our opinion, decarburization definitely plays a role but there is also contribution of kinetic effects because both DSC and vacuum sintering cycles are far from equilibrium during the heating ramp.

Regarding homogenization effects, new Fig. 3 (see answer to comment #1) proves the presence of large agglomerates of Ni and Fe. Moreover, C black additions (used for C control) are 4 times higher for Alloy C1 than for Alloy C2.

According to the referee's comments, if decarburization progresses as the DSC cycles are repeated, we should expect a change in the solidification range of Alloy C2, corresponding, for instance, to the precipitation of M6C and this is not the case. Therefore, we do not discard the effect of chemical homogenization as a possible factor affecting melting and solidification phenomena in our WC-Fe-Ni-Co-Cr3C2-carbon black mixtures.

In the revised text, we have considered the valuable referee's comments along with the explanation given in these paragraphs.

5.Analysis of the correlation between Thermocalc (TC) estimates and experimental values of the solidification range should be clarified (Figure 7 and Table 3). Why do the TC estimates not depend on the C content? Also it is not clear that the agreement between TC estimates and measured values of the solidification range is better for higher Cr content. In the legend of Figure 7, high C and low W mean the same thing. In Table 3, there is a contradiction between "Thermocalc estimates*" and the reference "*Obtained by Infrarred spectrometry". The 2 temperatures given for the DSC solidification peaks should be explained in the legend or in the table. The link between Figure 7 and Table 3 is not clear and should be commented.

Answer:

In the revised versions, Table 3 becomes Table 4 and Figure 7 changes to Fig. 9.
TC estimates do not depend on the C content because are only calculated for the C content measured by IR spectrometry after vacuum sintering in each compositions (last

column in new Table 4).

Taking this into account, we have estimated the solidification range given by TC® predictions for the measured C contents and compared them with the temperature intervals measured from DSC solification peaks (1st and 3rd cycles)

-In caption of new Fig. 9 “Low W” has been changed to “Low C”
-The asterisk in Thermocalc estimates has been removed.
-The reason for giving two temperatures in DSC solidification peaks in Table 4 is that correspond to the 1st DSC and 3rd DSC cycle respectively. This has been included in Table 4 heading.
-The link between new Fig. 9 and new Table 4 is as follows:

Thermocalc estimates are considered to be related to solidification DSC events because the system is closer to equilibrium conditions after being 10 min at 1450ºC. In addition, the C content measured by IR corresponds to sintered specimens after all decarburization phenomena related to carbothermal reduction of powder oxides. In all sintered specimens we have confirmed the absence of free C or M6C phases.

This has been included in the revised manuscript

6.The effect of Cr carbides as grain growth inhibitor is not clearly seen on the microstructures of Figure 10. The authors should comment on that point.

Answer:
WC grain growth inhibition by Cr additions is easily observed in submicron and ultrafine hardmetal grades. In this case, it is not that easy because we have selected a powder with large particle and grain size. The mean WC grain size is 3.7 microns according to the supplier. (see attached SEM image in the file included in pdf version).

WC grain growth in hardmetals is generally explained as a solution reprecipitation phenomena (Ostwald ripening), which is limited by 2D nucleation or nucleation on defects (See  Z. Roulon, J.M. Missiaen, S. Lay Int. J. Refract. Metals & Hard Mat. 86 (2020) 105088. These authors study the effect of binders alternative to cobalt on WC grain growth and show that growth in Fe based binders is much lower than in Co or Ni ones and that growth rate increases with the C activity. We have decided to include this reference in the revised text.

The same happens in our materials. There are no large differences between mean WC grain sizes of alloys with or without Cr, which is likely due to the fact that the selected WC powders were already large (that is, the original surface area, which is the driving force for the grain growth process, is low in the starting powders). Moreover, the dissolution of WC grains in Fe based binders is much slower than in Ni or Co based ones.
A comment has been included in the revised text regarding this point.

A few other details:
-Cr and C in title:

Answer: New title says “chromium and carbon” instead of Cr and C.

-Please check the sentence in introduction: "substitution of cobalt either by nickel or iron… both oxidation and corrosion resistance improve". You probably mean for nickel. Substitution by iron deteriorates corrosion resistance

Answer: Yes. This has been corrected.

-The sentence in section 3.1.a) "However, alloy C2 (with lower C activity) has only one at 1368ºC, that is, coinciding with the second peak observed in alloy C1 by with approx. double intensity" is not clear and should be rewritten.

Answer: The new text is as follows:
“However, alloy C2 (with lower C activity) has only one at 1368ºC. This temperature coincides with that of the second peak found in alloy C1. However, its intensity is aprox. 100% higher. This means that shrinkage begins at higher temperatures as C content decreases in these alloys but at a higher rate than that found in low C materials”

-"Some WC polygonal grains are found in alloy C1 (with no Cr and high C content), suggesting that rounded WC grains are formed by the grain growth inhibition effect of Cr along with the higher solubility of WC grains in the liquid phase as the C content decreases" : the end of the sentence (… along with…) should be clarified. If the authors mean that there is an effect of C content on the grain shape, they should specify.
Answer: We have explained this effect in more detail and combine it with the answer to comment #6.

The new text is as follows:

There are no large differences between mean WC grain sizes of alloys with or without Cr, which is likely due to the fact that the selected WC powders were already large (that is, the original surface area, which is the driving force for the grain growth process, is low in the starting powders). Moreover, the dissolution of WC grains in Fe based binders is much slower than in Ni or Co based ones [26]. This combined with the WC grain growht inhibition effect of chromium additions could explain the rounded morphology found for WC grains in most of these compositions (Fig. 12). The only exception is alloy C1, where some WC polygonal grains are found after sintering. This alloy has no chromium and high C content suggesting that, under these conditions, the observed shape change in WC crystals could be due to the activation of 2D nucleation phenomena described by several authors as responsible for to this anisotropic growth [26].

Answers to Reviewer # 2 comments:
1-: The paper presents an interesting study on the effect of Cr and C on the sintering of WC-Fe-Ni-Co-Cr, combining experimental results and thermodynamic calculations. Although it shows a good piece of work, supported by a good scientific discussion, there is an aspect that should be reviewed in the beginning of the discussion. In fact, the authors seem to neglect the relevant contribution of the initial solid state sintering for the densification of hardmetals, when they say, related to Fig. 1:"….peak observed in alloy C1 by with approx. double intensity. This means that shrinkage starts at higher temperatures for the allow with lower C content….". This is incorrect, since shrinkage starts at similar temperatures, ~1000ºC, Fig. 1, for both alloys by solid state sintering processes, only the contribution of LPS appears at lower temperatures for the alloy with higher C content.

Answer:  This question is similar to comment 1 of Reviewer#1. We just focused on liquid phase sintering phenomena and forgot to talk about the contribution of solid state sintering mechanisms. We thank the referee for noticing this.  Therefore, we have modified the text in order to include it along with two additional references [22 and 23 in the new version]. The new text is included at the beginning of Section 3.1. (a), in the part explaining Fig. 1.

2-Some figures should be improved:

(i)The dilatometric curves in Fig. 1a) and 3a) and b) show a final shrinkage that is not representative and should be removed; and why Fig 1c) has not the same scale as

1b)?

Answer: We have repeated some of these experiments and obtained the same results. So, we consider that Figs. 1a and 3a are representative of the materials behaviors. If the reviewer agrees, we would rather keep them in the revised version. As the different scales in Figs. 1b and 1c, this is because they show different magnitudes. Fig. 1b shows the shrinkage rate as a function of temperature and Fig. 1c shows differential scanning calorimetry curves corresponding to the same alloys.

(ii)The diagrams of Fig. 5 are not legible, the letters are very small, the lines of the axes are not visible and the designation of the phases could be simplified.

Answer: Letters in Fig. 5 have been modified in order to make it more visible. With all modifications made in the revised version, Figs. 4 and 5 have been renamed as Figs. 6 and 7.

(iii)In Table 2 it misses the indication of the values obtained during cooling: "**Data obtained from the cooling ramp"

Answer: This is a mistake. This table only includes data from the heating ramps. The text "**Data obtained from the cooling ramp" has been removed from Table 2. In addition, this table has been renamed as Table 3 in the revised version in order to answer referee's #1 questions.
Data obtained from the cooling ramp are included in new Table 4 in the revised version.

3-There are also some typos, namely in the title, and along the text to be corrected.

Answer: Typos and misspelling have been revised through the whole text to the best of our knowledge.

Answers to Reviewer # 2 comments:

| | |
|---|---|
| | 1-: The paper presents an interesting study on the effect of Cr and C on the sintering of WC-Fe-Ni-Co-Cr, combining experimental results and thermodynamic calculations. Although it shows a good piece of work, supported by a good scientific discussion, there is an aspect that should be reviewed in the beginning of the discussion. In fact, the authors seem to neglect the relevant contribution of the initial solid state sintering for the densification of hardmetals, when they say, related to Fig. 1:"….peak observed in alloy C1 by with approx. double intensity. This means that shrinkage starts at higher temperatures for the allow with lower C content….". This is incorrect, since shrinkage starts at similar temperatures, ~1000ºC, Fig. 1, for both alloys by solid state sintering processes, only the contribution of LPS appears at lower temperatures for the alloy with higher C content.<br><br>Answer: This question is similar to comment 1 of Reviewer#1. We just focused on liquid phase sintering phenomena and forgot to talk about the contribution of solid state sintering mechanisms. We thank the referee for noticing this. Therefore, we have modified the text in order to include it along with two additional references [22 and 23 in the new version]. The new text is included at the beginning of Section 3.1. (a), in the part explaining Fig. 1.<br><br>2-Some figures should be improved:<br><br>(i)The dilatometric curves in Fig. 1a) and 3a) and b) show a final shrinkage that is not representative and should be removed; and why Fig 1c) has not the same scale as 1b)?<br>Answer: We have repeated some of these experiments and obtained the same results. So, we consider that Figs. 1a and 3a are representative of the materials behaviors. If the reviewer agrees, we would rather keep them in the revised version. As the different scales in Figs. 1b and 1c, this is because they show different magnitudes. Fig. 1b shows the shrinkage rate as a function of temperature and Fig. 1c shows differential scanning calorimetry curves corresponding to the same alloys.<br><br>(ii)The diagrams of Fig. 5 are not legible, the letters are very small, the lines of the axes are not visible and the designation of the phases could be simplified.<br>Answer: Letters in Fig. 5 have been modified in order to make it more visible. With all modifications made in the revised version, Figs. 4 and 5 have been renamed as Figs. 6 and 7.<br><br>(iii)In Table 2 it misses the indication of the values obtained during cooling: "**Data obtained from the cooling ramp"<br>Answer: This is a mistake. This table only includes data from the heating ramps. The text "**Data obtained from the cooling ramp" has been removed from Table 2. In addition, this table has been renamed as Table 3 in the revised version in order to answer referee's #1 questions.<br>Data obtained from the cooling ramp are included in new Table 4 in the revised version.<br><br>3-There are also some typos, namely in the title, and along the text to be corrected.<br><br>Answer: Typos and misspelling have been revised through the whole text to the best of our knowledge. |

April 11th, 2020

Dear Editor:

We would like to submit the article entitled “Effect of Cr anc C contents on the sintering of WC-Fe-Ni-Co-Cr multicomponent alloys” for publication in the International Journal of Refractory Metals and Hard Materials. Please, do not hesitate to contact us if you have any questions.

Yours sincerely,

J.M. Sánchez

CEIT-IK4 . Paseo Manuel de Lardizabal, 15, 20018, San Sebastián, Spain.

phone: 34-943-212800
fax:34-943-213076
email: jmsanchez@ceit.es

**Ref: IJRMHM-D-20-00205**

**Title: Effect of Cr anc C contents on the sintering of WC-Fe-Ni-Co-Cr multicomponent alloys**

**Journal: International Journal of Refractory Metals and Hard Materials**

**Answers to Reviewer # 1 comments:**

1- **Authors should give details about the powders used, especially the particle size. A micrograph of a powder compact would be useful to appreciate the heterogeneity in the powder mixtures, which is the reason given by the authors for the broad temperature range of liquid formation.**

Answer: We definitely agree with the referee's comment. In the new version, we have included a new Table 1 at the beginning of section 2 with the particle size of starting powders. We have also included a new Fig. 3 corresponding to a green compact of composition C4 (medium C content) (see new Table 2). A paragraph has been included in Section 3.1(a) of the revised version that provides the requested information about the scale of microstructural segregation in the green compacts.

2. **The authors state that sintering starts at higher temperatures for the W-rich alloys. But from the dilatometric plots, it appears that sintering (apparently solid state sintering) starts at a lower temperature for these alloys. This is indeed a classical result of solid state sintering of WC-Co alloys which has been observed by several authors, and is probably related to a better solid state spreading of the binder due to a lower interface energy in W-rich alloys (see e.g. A. Petersson, Int. J. Refractory Metals & Hard Materials 22(4-5), 2004, 211-217). The authors probably mean that the liquid phase sintering peak is delayed to higher temperatures for the W-rich alloys but this should be clarified.**

Answer: Yes. Our intention was to describe melting phenomena and not shrinkage in solid state. Again, we thank the referee for the comment. We have modified the text in order to include solid state sintering effects along with two additional references [22 and 23 in the new version]. The new text is included at the beginning of Section 3.1. (a), in the part explaining Fig. 1.

3. **The authors should be careful when relating the area of endothermic peaks to the amount of liquid, since the composition may influence the enthalpy of melting. And from figure 1 c), I would not say that area of the endothermic peak on cooling is 100% higher for the C2 alloys, since the peak for C1 alloy is broader. Did they make a measurement or is this a rough estimate?**

Answer: After the reviewer's comment, we have revised the calculation of DSC peak areas and found that the melting range we considered for Alloy C1 was only from 1300ºC to 1380ºC. We agree that there is some liquid above 1261ºC. Considering this, the area under the DSC peak of Alloy C1 (High C) for the first heating event is still 30% lower than that calculated for alloy C2

(Low C). We have also corrected the areas corresponding to exothermic peaks, which are also higher for Alloy C2 than for Alloy C1, but only by 20%.

The theory behind the calculation of the amount of liquid assumes that melting occurs in equilibrium conditions (which is also an approximation). In such a case:

$$dQ = \Delta H_f(T) \cdot dm_L \quad \textbf{[1]}$$

where *Q* is the heat provided to the sample during the melting process, $m_L$ is the liquid mass in thermodynamic equilibrium, $\Delta H_f(T)$ is the amount of heat required to melt a gram of the sample at temperature *T*. Taking the derivative of *dQ* with respect to time:

$$\frac{dQ}{dt} = \Delta H_f(T) \cdot \frac{dm_L}{dt} \quad \textbf{[2]}$$

and *dQ/dt* is the heat flux rate ($\phi_m$) measured by DSC with minus sign:

$$-\phi = \Delta H_f(T) \cdot \frac{dm_L}{dt} \quad \textbf{[3]}$$

Clearing $dm_L$ and integrating with respect to temperature:

$$dm_L = \frac{-\phi}{\Delta H_f(T)} dt = \frac{-\phi}{\Delta H_f(T)} \cdot \frac{dT}{\beta} \quad \textbf{[4]}$$

$$m_L = \int_{T_i}^{T} \frac{-\phi}{\beta \cdot \Delta H_f(T)} dT \quad \textbf{[5]}$$

where $\beta$ is the heating rate (10°C/min in our case).

Extending the interval to the end of the DSC peak ($T = T_f$), and the total amount of liquid "*m*" is given by:

$$m = \int_{T_i}^{T_f} \frac{-\phi}{\beta \cdot \Delta H_f(T)} dT \quad \textbf{[6]}$$

The term $A = \int_{T_i}^{T_f} \frac{-\phi}{\beta} dT$ corresponds to the area enclosed by the considered DSC peak.

We have also revised the bibliography to the best of our knowledge and have not found information regarding the enthalpies of melting for Fe-Ni-Co-Cr-W alloys. Therefore, the correlation between areas of DSC peaks and actual liquid contents is only qualitative.
The method for calculating DSC peak areas and this final comment have been included in the revised text.

4. **More important, the authors explain the effect of C content on the temperature of liquid formation by homogenization of the metallic binder composition. They argue**

**that a Fe-rich liquid would form at lower temperature for C-rich alloys. But I do not understand the reason why this Fe-rich liquid would form rather in C-rich rather than in W-rich alloys. In addition, for a binder with uniform composition, the solidus temperature increases when decreasing the C content, as predicted by the phase diagrams (see Fig. 6) and this must have a first-order effect on the temperature of liquid formation, before incriminating a metallic composition gradient in the binder. Finally, the DSC plots after several runs show the same position for the peaks for alloys C1 and C2 on heating and on cooling, which suggests a decarburization of the alloys and a liquid formation which could correspond to the eutectic liquid on the W-rich side of the 2-phase domain for both compositions (see Fig. 6).This decarburization is often an issue with the small samples used in DSC (1 mm3 here) for long or repeated thermal cycles. This discussion of the C content effect on the temperature of liquid formation should be rewritten by taking these remarks into consideration.**

Answer: Of course, we agree with the referee's comment about the displacement of melting onset to higher temperatures as C activity decreases. This is a well-known effect in cemented carbides and, as the referee points out, is clearly reflected in Thermocalc ® calculations.

We also agree on considering decarburization effects, although it is impossible to measure carbon contents in DSC samples owing to their small size. Repeated DSC experiments were carried out without opening the furnace chamber and always protected with pure Argon atmosphere (nominal oxygen and water contents in this gas are 2 ppm and 3 ppm respectively). Of course, the procedure includes leak testing and 3 purges of the calorimeter chamber to remove all residual air (the whole process takes 1. 5 hours). Main decarburization should be expected for the first DSC heating cycle due to carbothermal reduction of oxides present in the powder mixtures. In repeated DSC experiments, the samples have already a high degree of sintering. Therefore, the specimen surface area is considerably reduced and decarburization kinetics should be slower.

Anyhow, although samples can be decarburized during repeated DSC experiments, melting and solidification temperature intervals observed experimentally are very different from those calculated by Thermocalc ® with TCFE10 database. The isopleth of new Fig. 2; including both compositions C1 and C2, shows that the melting range of alloys near the upper C side of the 2 phase domain has a maximum value of 69$^{o}$C (far from the 122$^{o}$C measured experimentally for Alloy C1). On the lower C side, the melting range corresponding with no presence of $M_6C$ is only 9$^{o}$C. Again, far from the 51$^{o}$C measured experimentally for Alloy C2.
In our opinion, decarburization definitely plays a role but there is also contribution of kinetic effects because both DSC and vacuum sintering cycles are far from equilibrium during the heating ramp.

Regarding homogenization effects, new Fig. 3 (see answer to comment #1) proves the presence of large agglomerates of Ni and Fe. Moreover, C black additions (used for C control) are 4 times higher for Alloy C1 than for Alloy C2.

According to the referee's comments, if decarburization progresses as the DSC cycles are repeated, we should expect a change in the solidification range of Alloy C2, corresponding, for instance, to the precipitation of $M_6C$ and this is not the case. Therefore, we do not discard the effect of chemical homogenization as a possible factor affecting melting and solidification phenomena in our WC-Fe-Ni-Co-$Cr_3C_2$-carbon black mixtures.

In the revised text, we have considered the valuable referee's comments along with the explanation given in these paragraphs.

**5. Analysis of the correlation between Thermocalc (TC) estimates and experimental values of the solidification range should be clarified (Figure 7 and Table 3). Why do the TC estimates not depend on the C content? Also it is not clear that the agreement between TC estimates and measured values of the solidification range is better for higher Cr content. In the legend of Figure 7, high C and low W mean the same thing. In Table 3, there is a contradiction between "Thermocalc estimates*" and the reference "*Obtained by Infrarred spectrometry". The 2 temperatures given for the DSC solidification peaks should be explained in the legend or in the table. The link between Figure 7 and Table 3 is not clear and should be commented**.

Answer:

In the revised version, Table 3 becomes Table 4 and Figure 7 changes to Fig. 9.
TC estimates do not depend on the C content because are only calculated for the C content measured by IR spectrometry after vacuum sintering in each compositions (last column in new Table 4).

Taking this into account, we have estimated the solidification range given by TC® predictions for the measured C contents and compared them with the temperature intervals measured from DSC solification peaks (1st and 3rd cycles)

- In caption of new Fig. 9 "Low W" has been changed to "Low C"
- The asterisk in Thermocalc estimates has been removed.
- The reason for giving two temperatures in DSC solidification peaks in Table 4 is that correspond to the 1st DSC and 3rd DSC cycle respectively. This has been included in Table 4 heading.
- The link between new Fig. 9 and new Table 4 is as follows:

  Thermocalc estimates are considered to be related to solidification DSC events because the system is closer to equilibrium conditions after being 10 min at 1450ºC. In addition, the C content measured by IR corresponds to sintered specimens after all decarburization phenomena related to carbothermal reduction of powder oxides. In all sintered specimens we have confirmed the absence of free C or $M_6C$ phases.

  This has been included in the revised manuscript

**6. The effect of Cr carbides as grain growth inhibitor is not clearly seen on the microstructures of Figure 10. The authors should comment on that point.**

Answer:
WC grain growth inhibition by Cr additions is easily observed in submicron and ultrafine hardmetal grades. In this case, it is not that easy because we have selected a powder with large particle and grain size. The mean WC grain size is 3.7 microns according to the supplier. (see attached SEM image).

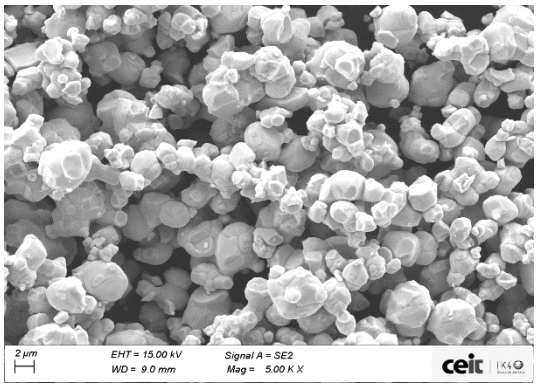


WC grain growth in hardmetals is generally explained as a solution reprecipitation phenomena (Ostwald ripening), which is limited by 2D nucleation or nucleation on defects (See Z. Roulon, J.M. Missiaen, S. Lay Int. J. Refract. Metals & Hard Mat. 86 (2020) 105088). These authors study the effect of binders alternative to cobalt on WC grain growth and show that growth in Fe based binders is much lower than in Co or Ni ones and that growth rate increases with the C activity. We have decided to include this reference in the revised text.

The same happens in our materials. There are no large differences between mean WC grain sizes of alloys with or without Cr, which is likely due to the fact that the selected WC powders were already large (that is, the original surface area, which is the driving force for the grain growth process, is low in the starting powders). Moreover, the dissolution of WC grains in Fe based binders is much slower than in Ni or Co based ones.
A comment has been included in the revised text regarding this point.

A few other details:

- Cr and C in title:

  Answer: New title says “chromium and carbon” instead of Cr and C.

- Please check the sentence in introduction: "substitution of cobalt either by nickel or iron… both oxidation and corrosion resistance improve". You probably mean for nickel. Substitution by iron deteriorates corrosion resistance

  Answer: Yes. This has been corrected.

- The sentence in section 3.1.a) "However, alloy C2 (with lower C activity) has only one at 1368ºC, that is, coinciding with the second peak observed in alloy C1 by with approx. double intensity" is not clear and should be rewritten.

  Answer: The new text is as follows:
  “However, alloy C2 (with lower C activity) has only one at 1368ºC. This temperature coincides with that of the second peak found in alloy C1. However, its intensity is aprox. 100% higher. This means that shrinkage begins at higher temperatures as C content decreases in these alloys but at a higher rate than that found in low C materials”

- "Some WC polygonal grains are found in alloy C1 (with no Cr and high C content), suggesting that rounded WC grains are formed by the grain growth inhibition effect of Cr along with the higher solubility of WC grains in the liquid phase as the C content decreases" : the end of the sentence (… along with…) should be clarified. If the authors mean that there is an effect of C content on the grain shape, they should specify.

Answer: We have explained this effect in more detail and combine it with the answer to comment #6.

The new text is as follows:

There are no large differences between mean WC grain sizes of alloys with or without Cr, which is likely due to the fact that the selected WC powders were already large (that is, the original surface area, which is the driving force for the grain growth process, is low in the starting powders). Moreover, the dissolution of WC grains in Fe based binders is much slower than in Ni or Co based ones [26]. This combined with the WC grain growht inhibition effect of chromium additions could explain the rounded morphology found for WC grains in most of these compositions (Fig. 12). The only exception is alloy C1, where some WC polygonal grains are found after sintering. This alloy has no chromium and high C content suggesting that, under these conditions, the observed shape change in WC crystals could be due to the activation of 2D nucleation phenomena described by several authors as responsible for to this anisotropic growth [26].

**Answers to Reviewer # 2 comments:**

**1- : The paper presents an interesting study on the effect of Cr and C on the sintering of WC-Fe-Ni-Co-Cr, combining experimental results and thermodynamic calculations.**

**Although it shows a good piece of work, supported by a good scientific discussion, there is an aspect that should be reviewed in the beginning of the discussion. In fact, the authors seem to neglect the relevant contribution of the initial solid state sintering for the densification of hardmetals, when they say, related to Fig. 1:"….peak observed in alloy C1 by with approx. double intensity. This means that shrinkage starts at higher temperatures for the allow with lower C content….". This is incorrect, since shrinkage starts at similar temperatures, ~1000ºC, Fig. 1, for both alloys by solid state sintering processes, only the contribution of LPS appears at lower temperatures for the alloy with higher C content.**

Answer: This question is similar to comment 1 of Reviewer#1. We just focused on liquid phase sintering phenomena and forgot to talk about the contribution of solid state sintering mechanisms. We thank the referee for noticing this. Therefore, we have modified the text in order to include it along with two additional references [22 and 23 in the new version]. The new text is included at the beginning of Section 3.1. (a), in the part explaining Fig. 1.

**2- Some figures should be improved:**

**(i) The dilatometric curves in Fig. 1a) and 3a) and b) show a final shrinkage that is not representative and should be removed; and why Fig 1c) has not the same scale as 1b)?**

Answer: We have repeated some of these experiments and obtained the same results. So, we consider that Figs. 1a and 3a are representative of the materials behaviors. If the reviewer agrees, we would rather keep them in the revised version. As the different scales in Figs. 1b and 1c, this is because they show different magnitudes. Fig. 1b shows the shrinkage rate as a function of temperature and Fig. 1c shows differential scanning calorimetry curves corresponding to the same alloys.

**(ii) The diagrams of Fig. 5 are not legible, the letters are very small, the lines of the axes are not visible and the designation of the phases could be simplified.**

Answer: Letters in Fig. 5 have been modified in order to make it more visible. With all modifications made in the revised version, Figs. 4 and 5 have been renamed as Figs. 6 and 7.

**(iii) In Table 2 it misses the indication of the values obtained during cooling: "**Data obtained from the cooling ramp"**

Answer: This is a mistake. This table only includes data from the heating ramps. The text "**Data obtained from the cooling ramp" has been removed from Table 2. In

addition, this table has been renamed as Table 3 in the revised version in order to answer referee's #1 questions.
Data obtained from the cooling ramp are included in new Table 4 in the revised version.

**3- There are also some typos, namely in the title, and along the text to be corrected.**

Answer: Typos and misspelling have been revised through the whole text to the best of our knowledge.

## HIGHLIGHTS

1- Cr alloying of WC-6wt.%%Fe-6wt%Ni-3wt.%Co alloys has been investigated for different C contents.

2- Homogenization of the chemical composition of the binder phase is faster the lower the C content of the alloy.

3- Although, Fe-Ni-Co (40/40/20) alloy is austenitic, BCC phases are partially stabilized in the binder phase for low C and high Cr contents.

4- Precipitation of submicron Cr-rich carbides precipitate at the WC-metal interface is avoided in the alloy with 0.75 wt.%Cr and 5.31 wt.%C.

# Effect of chromium and carbon contents on the sintering of WC-Fe-Ni-Co-Cr multicomponent alloys

T. Soria-Biurrun[1,2], L. Lozada-Cabezas[1,2], F. Ibarreta-Lopez[3], R. Martinez-Pampliega[3], J.M. Sanchez-Moreno[1,2]

1- CEIT-Basque Research and Technology Alliance (BRTA), Manuel Lardizabal 15, 20018 Donostia / San Sebastián, Spain.
2- Universidad de Navarra, Tecnun, Manuel Lardizabal 13, 20018 Donostia / San Sebastián, Spain.
3- FMD CARBIDE, Fabricación Metales Duros, S.A.L.,Gudarien etorbidea, 18,48970 Basauri, Spain

**Abstract**

WC-Fe-Ni-Co-Cr cemented carbides have been obtained by liquid phase sintering from WC-Fe-Ni-Co-$Cr_3C_2$ powder mixtures. Taking the 40wt.%Fe-40wt.%Ni-20wt.%Co alloy as a reference, new binder phases has been prepared by introducing controlled amounts of Cr and C, via $Cr_3C_2$ and C black powders respectively. As described for WC-Co-Cr materials, Cr additions are observed to reduce the eutectic temperatures of the WC-Fe-Ni-Co system. First liquids detected on heating exhibit wide temperature melting ranges, which become narrower and are displaced to higher temperatures on repeated heating and cooling cycles. Apart from the decarburization associated to the carbothermal reduction of powder oxides, this phenomenon could be also associated to the homogeneization of the chemical composition of these multicomponent binder phases, which is faster as C content decreases. Correlation between experimental melting and solidification temperature ranges and those predicted by Thermocalc® is better as Cr content increases. Experimental C windows, defined in this work by the absence of free C or η phases, are located at C contents higher than those estimated by Thermocalc®. Although the 40wt.%Fe-40wt.%Ni-20wt.%Co alloy is austenitc, BCC phases are partially stabilized at low C and high Cr contents. Although these compositions are free from η phases or free C, a precipitation of Cr-rich carbides is found at the WC-metal interface. These precipitates are not observed in the alloy with 0.75 wt.% Cr (i.e. 5 wt.% of the nominal metal content) and 5.39 wt.%C. This C content is 0.17 wt.% higher than that predicted for precipitation of $M_7C_3$.

## 1. Introduction

The need for cobalt replacement in hardmetals has been historically associated to potential health issues [1-3]. However, at present, it is driven by the risk of supply due to its increasing use in Li-ion batteries for the automotive industry [4,5]. It is well known that total substitution of cobalt either by nickel or iron leads to lower hardness and fracture strength values, although both oxidation and corrosion resistance improve in the case of chromium additions [6-8]. Moreover, in the case of WC-Fe alloys, the width of the so-called "carbon window" (i.e. the carbon range without precipitation of either free C or secondary carbides) is significantly reduced. Therefore, it is very difficult to produce components from WC-Fe materials at industrial scale. According to different authors, larger carbon windows are obtained by combining Fe, Ni and Co, especially for compositions within the austenitic range [9,10]. Among them, the alloy consisting of 40wt.%Fe-40wt.%Ni-20wt.%Co is one of the most promising due to its relatively wide C window and its high toughness compared with other Fe-Ni-Co based compositions [9]. Alternatively, recent works have been focused on using high entropy alloys (HEA) as Co substitutes in hardmetals [11-14]. Examples of these materials include combinations of Fe, Ni, Co, Cr, Cu and even Al, where at least, 5 of these elements are present with near equiatomic ratios. Due to their high configurational entropy, these alloys are expected to present very high chemical stability at high temperatures, provided that all elements form a single solid solution phase [11,14]. The design of such alloys is a challenging task since both thermodynamic studies and sintering experiments confirm the precipitation of undesired phases when sintered in combination with tungsten carbide. This is the case of compositions with high Cr contents, where precipitation of $M_7C_3$ and other Cr-rich carbides cannot be avoided for any carbon content [15-18]. Moreover, no data have been found on critical properties as the solubility of chromium in the binder phase of WC-Fe-Ni-Co alloys, which also contains differents amounts of tungsten depending on the total carbon activity.

As mechanical properties are concerned, very little information is published about fracture strength and toughness of cermets or cemented carbides with multicomponent binder phases. According to Chen et al. [19], toughness values of WC-HEA cemented carbides are in the range of those reported for standard hardmetals ($K_{1C}$=17.4 MPa.√m for 20 wt.% binder content). However, their processing and testing methods are far from standard procedures and more data are needed to confirm these promising results. In the case of HEA cermets, toughness is clearly below that of standard TiCN cermets with $K_{1C}$ values between 4 to 7 MPa.√m for the same binder contents [20]. Taking this into account, a deeper investigation is clearly needed in order to understand the correlation between these new microstructures

and the achivable mechanical properties. The present work is focused on WC-Fe/Ni/Co (40/40/20 in wt.%) alloys, where C windows are wide enough for industrial processing. The objetive is to study the changes induced by Cr alloying not only on the C window but also on the sinterability of these materials.

## 2. Experimental procedure

The mean particle size of as-received powders is included in Table 1. Over 50 different compositions have been prepared with these materials in order to define with precision the compositional ranges free of precipitation of undesired phases. A selection of 9 alloys corresponding to the upper and lower bounds of the corresponding C windows are included in Table 1. The metal content was selected to be 15 ± 1 wt.%, corresponding approximately to 26 ± 1 vol.%, similar to that of cobalt in WC-15 wt.% Co alloys, which were taken as reference. As previously explained, the ratio between Fe, Ni and Co was 40/40/20 (in wt.%) in all cases. Cr additions were carried out via $Cr_3C_2$ carbide and the C content was modified by including either carbon black or tungsten powders in the mixtures. Mixing/milling was made in a planetary equipment at 100 rpm for 5 hours using ethanol as liquid media and a ball to powder ratio of 6 (in wt.). Paraffin, used as pressing aid, was added in the last milling hour. Afterwards, the powders were dried for 40 min at atmospheric pressure in a thermostatic bath (80+/-2ºC). Green compacts were obtained by double action pressing at 160 MPa. The equipment used in dilatometric experiments was a Netzsch TA 402 E/7 and that used in differential scanning calorimetric tests was a TGA/DSC Setaram Setsys Evolution 16/18. Dilatometric specimens were cylinders with both height and diameter of 5 mm. DSC samples were cubes of aprox. 1 mm side. The heating cycle was the same in both types of experiments. It consisted of a heating ramp of 10ºC/min up to 1450ºC. Dwelling time at this temperature was 10 min. Argon at atmospheric pressure was used as a protective atmosphere. Temperatures $T_i$ and $T_f$ correspond to the upper and lower bounds of the melting range of each DSC peak respectively and were determined by using the SETSOFT software [21]. This software also allows for the calculation of peak areas ($A$):

$$A = \int_{T_i}^{T_f} \frac{-\phi}{\beta} dT \qquad \text{(eq. 1)}$$

where $\phi$ is" the heat flux rate, and "$\beta$" is the heating rate.

As it is well known, the enthalpy of melting ($\Delta H_f(T)$) is needed to calculate the amount of liquid produced during DSC experiments:

$$m = \int_{T_i}^{T_f} \frac{-\phi}{\beta \cdot \Delta H_f(T)} dT \qquad \text{(eq. 2)}$$

No $\Delta H_f(T)$ values are available in the literature for the combination of metals studied in this work (i.e. FeNiCoCrW alloys). Estimations of the amount of liquid generated during sintering are based on comparing the corresponding DSC areas and, therefore, are only qualitative. In all cases, the heating and cooling cycles was repeated thrice. The idea was to analyze how melting and solidification events change during the binder phase alloying process. Afterwards, standard vacuum sintering experiments were carried out in a industrial furnace with graphite heating elements at a heating rate of 10ºC/min up to 1450ºC. The vacuum level used during this step was $10^{-2}$ mbar. Above this temperature, the pressure was increased to 100 mbar by introducing argon in the furnace chamber and maintained during the 1 h sintering plateau. C contents were measured by means of infrared spectrometry both in green compacts and sintered materials. Standard ISO 3369 was used for density measurements. Finally, the sintered specimens were ground and polished down to 1 µm diamond paste for microstructural analysis, which was carried out by optical and scanning electron microscopy (FEG-SEM) and energy dispersive X-ray spectroscopy (EDS). Phase identification was carried out by X-Ray diffraction (XRD) (with Ni-filtered CuKα radiation) using Bragg-Brentano configuration. Vickers hardness was determined with 30 kg of applied load at room temperature.

## 3. Results and discussion

### 3.1. Thermal analyses: dilatometry and calorimetry

(a) WC-FeNiCo (40/40/20) reference alloys

As seen in Fig. 1, carbon activity has a significant effect on the shrinkage of WC-FeNiCo (40/40/20) alloys. The shrinkage rate of alloy C1 (with higher C content) exhibits two different peaks at 1337ºC and 1369ºC. However, alloy C2 (with lower C activity) has only one at 1368ºC. This temperature coincides with that of the second peak found in alloy C1. However, its intensity is aprox. 100% higher. This means that shrinkage begins at higher temperatures as C content decreases in these alloys but at a higher rate than that found in low C materials.

Shrinkage onset occurs at lower temperatures in the low C alloy (i.e. C2), which agrees with previous dilatometric data carried out on WC-Co alloys [22,23]. According to these authors, densification

is related to solid state spreading of the binder, which is enhanced in low carbon WC-Co alloys due to their lower interface energy. As temperature increases above 1300ºC, shrinkage acceleration is much higher in the high C alloy (C1), which, according to DSC data (Fig. 1c), is related to the presence of a liquid phase. Liquid formation is delayed in the case of alloy C2, but when it happens leads to a higher total shrinkage. DSC data show that liquid formation occurs in a much wider temperature range for alloy C1 than for alloy C2: 122ºC and 51ºC respectively. Moreover, the area enclosed by these DSC endothermic peaks, calculated using eq. 1, is 32% higher for Alloy C2 than for Alloy C1 (20.26 J/g vs. 15.27 J/g respectively). Areas of exothermic peaks found on cooling are only 21% higher for Alloy C2 than for Alloy C1 (25.7 and 21.2 J/g respectively). These data suggest that a higher amount of liquid could be present in the alloy with lower C content. Therefore, the significant shrinkage acceleration observed during the heating ramp of the dilatometric cycle could be due to larger contribution of rearrangement mechanisms during liquid phase sintering.

It is also worth noting that exothermic peaks detected in the cooling ramp are narrower than endothermic peaks found on heating. Considering Thermocalc® calculations carried out with TCFE10 database, these results suggest that certain decarburization occurs during the DSC cycle (Fig. 2). Nevertheless, the melting range calculated for the upper carbon limit of the 2 phase domain is of 69ºC (far from the 122ºC measured experimentally for Alloy C1). On the lower C side, the melting range corresponding with no presence of $M_6C$ is only 9ºC. Again, far from the 51ºC measured experimentally for Alloy C2. Thus, although decarburization definitely plays a role on melting and solidification events, there is also contribution of kinetic effects, since DSC cycles are far from equilibrium conditions. Homogenization of the chemical composition of the binder phase could be the cause of this discrepancy between experiments and thermodynamic calculations.

The scale of microstructural segregation can be estimated by EDS mapping performed on the surface of green compacts (Fig.3). These analysees confirm the presence of Fe and Ni agglomerates with sizes ranging from 8 to 20 μm. Although, it is not perceptible in these images, it is also worth mentioning that composition C1 contains four times more black carbon addition than Alloy C2.

Repeated DSC experiments on specimens of Alloy C1 show that endothermic peaks become narrower and shifted towards higher temperatures as the cycle is repeated once and twice (Fig. 4a). The same happens with solidification peaks, but, in this case, there is not much difference between those corresponding to the second and the third DSC cycles. Again, this can be related to the contribution of decarburization and homogenization phenomena. In the case of Alloy C2 (Fig. 4b),

melting peaks also become narrower on repeated heating and cooling, but, in this case, the temperatures corresponding to both endothermic and exothermic peaks do not change. If decarburization progressed during 2nd and 3rd DSC cycles, there should be a change in the solidification interval associated to the precipitation of $M_6C$ at higher temperatures (see. Fig. 2). Therefore, this could indicate that the carbon content has not changed and the composition of the binder phase in Alloy C2 is already homogeneous after the first DSC cycle.

(b) Chromium alloying of WC-FeNiCo (40/40/20) materials

As seen in Table 2, the Cr contents selected in this study range from 0.75 to 2 wt.% Cr (corresponding to 5 to 12 wt.% with respect to the nominal Fe+Ni+Co+Cr content). The effects of such additions on shrinkage and shrinkage rate curves are shown in Fig. 5. Again, the effect of C content is to be taken into account.

Thus, in high C alloys (Figs. 5a and 5b), chromium additions tend to increase the total shrinkage after sintering. The shape of shrinkage rate graphs vs. temperature change from composition C6 (with 1 wt.% Cr) in which only one asymmetric peak is observed (with the minimum located at 1340ºC) to composition C8 (with 2 wt.% Cr), in which two shrinkage rate peaks are clearly distinguished. These peaks appear shifted towards lower temperatures as Cr content increases, which is consistent with that reported for WC-Co-Cr alloys, where Cr additions are found to reduce the melting temperatures by more than 100ºC [24]. This is also the case in WC-FeNiCoCr alloys, as confirmed by DSC experiments (Table 3 and Figs. 6 and 7). These data prove that liquid appears at 1200ºC-1218ºC in the alloys with 1 and 2 wt.% Cr content (C6 and C8), but not in Alloy C3 (with 0.75wt%Cr), where melting onset is detected at ≈ 1290ºC. Therefore, a minimum Cr seems to be needed to form enough liquid around 1200ºC in this system. This indicates that Cr becomes less available for liquid formation as it is dissolved in the FeNiCo binder phase. As described in the previous section, this dissolution process can be studied by analyzing the changes of DSC peaks after repeated heating and cooling DSC cycles. Again, only one melting event is detected after the 3rd DSC cycle in all cases indicating that the compositions of their binder phases have been homogenized. As described for the alloys without Cr, peaks obtained after 3 repeated DSC cycles are narrower and shifted towards higher temperatures and no Cr rich eutectics are present in any of the studied systems.

In low C alloys, the total shrinkage does not show a clear trend with the Cr content (Fig. 5c). The maximum total shrinkage is obtained for alloy C7 (16.4%), whereas C5 (with half the Cr content of C7)

and C9 (with double Cr content) only reach 13.0% and 14.7% respectively. Shrinkage rate curves show that, in these two latter cases, shrinkage deccelerates sharply once the peak is exceeded, contrary to what happens in high C compositions (compare Figs. 5b and 5d).

DSC experiments carried out on low C materials show that the eutectic found between 1200ºC and 1218ºC in high C compositions disappears in composition C7 (twin of C6 but with low C) and is displaced to higher temperatures in alloy C9 (twin of C8 but with low C) (see Figs. 6 and 7). These phenomena suggest that, when C activity decreases, $Cr_3C_2$ carbide powders are more prone to dissolve in the binder phase of WC-FeNiCo (40/40/20) materials than to be involved in low eutectic reactions.

Table 4 includes the temperature ranges of solidification measured for the 1st and 3rd DSC cycles for each WC-FeNiCoCr alloy. Solidification ranges estimated by Thermocalc ® (TCFE 10 database) are also included along with C windows defined by the only presence of WC (MC_SHP) and FCC_A1 phases (Figs. 8 and 9). Thermocalc estimates are considered to be better related to solidification DSC events because the system is closer to equilibrium conditions after being 10 min at 1450ºC. In addition, the C content measured by IR corresponds to sintered specimens after all decarburization phenomena related to carbothermal reduction of powder oxides. The absence of free C or $M_6C$ phases was confirmed in all sintered specimens. Taking this into account, these data show that correlation between TC® estimations and experimental values is better as the Cr content increases within the studied range. For lower Cr contents, estimations are clearly below experimental data.

### 3.2. Vacuum sintering experiments

Samples sintered in vacuum were used for microstructural analyses and the determination of the total C content by means of infrarred spectrometry. As described in the experimental procedure over 50 compositions were studied in order to determine the experimental C windows. Comparison of these values with theoretical predictions carried out by TC® software show a reasonable agreement in the widths of C windows. However, in all cases, the experimental ones are displaced towards higher C contents. Typical C windows, defined by the absence of free C and $\eta$ phases, are now narrower due to the precipitation of Cr-rich $M_7C_3$ carbides (Fig. 8).

Density values are, in all cases, above 99% T.D.. According to ISO 4499-4 standard, porosity in C1 and C2 alloys ranges from A00-B00-C00 to A02-B04-C00. In Alloys with 2wt.%Cr, porosity goes from A02-B02-C00 in high C compositions (alloy C8) to A04-B04-C00 in low C ones (alloy C9).

Identification of crystalline phases in vacuum sintered samples has been carried by X-ray diffraction (Fig. 10). Only austenite (FCC) and ferrite (BCC) peaks are identified as constituents of the binder phase, the rest correspond to the WC phase. This means that other carbides, if present, are below the XRD detection level (≈ 1 vol%). The FCC to BCC ratios, estimated by the direct comparison method [25], show that most high C alloys have austenite as the major constituent of the binder phase (Fig. 11). This is due to the well known FCC stabilizing effect of both C and Ni in Fe based alloys. On the contrary, a higher amount of BCC phase is found in low C alloys with Cr additions, which is due to the BCC phase stabilizer effect of Cr in Fe alloys. In the case of alloy C6 (with 1wt.%Cr), C content after sintering is not high enough to stabilize the FCC phase.

XRD analyses have been complemented with scanning electron microscopy to confirm the absence of free C and η phases (Fig. 12). There are no large differences between mean WC grain sizes of alloys with or without Cr, which is likely due to the fact that the selected WC powders were already large (that is, the original surface area, which is the driving force for the grain growth process, is low in the starting powders). Moreover, the dissolution of WC grains in Fe based binders is much slower than in Ni or Co based ones [26]. This combined with the WC grain growht inhibition effect of chromium additions could explain the rounded morphology found for WC grains in most of these compositions (Fig. 12). The only exception is alloy C1, where some WC polygonal grains are found after sintering. This alloy has no chromium and high C content suggesting that, under these conditions, the observed shape change in WC crystals could be due to the activation of 2D nucleation phenomena described by several authors as responsible for to this anisotropic growth [26].

At higher magnification, SEM images also show that submicron Cr-rich carbides precipitate in alloys C8 and C9 (with 2 wt.%Cr), mainly at WC-binder interfaces (Fig. 13). Detailed EDS mappings show that these carbides may contain Fe and Co but not Ni. These carbides are also identified in compositions C6 and C7(both with 1wt.%Cr), but are less frequent.

Finally, in alloys with 0.75 wt.% Cr (i.e. C3, C4 and C5), only the one with higher C content (C3) contains Cr-rich carbides, being Alloys C4 and C5 free of them (Fig. 14). Their C contents are 5.39 and 5.31 wt.% respectively (Table 4), which are 0.09 and 0.17% wt.% higher that those calculated by Thermocalc ® for $M_7C_3$ precipitation (≈ 5.22 wt.% C). Anyhow, qualitative trends are in good agreement and consistent with thermal analyses, suggesting that the solubility limit of Cr in Fe-Ni-Co (40/40/20) alloys depends critically on the C activity. It is also possible that these phases could be dissolved in subsequent thermal

treatments, although in vacuum sintering cycles the dwelling time at 1450ºC was 6 times longer than in DSC tests. TEM work is being carried out to determine the crystallographic nature of these precipitates.

## 4. Conclusions

Chromium alloying of WC-6wt.%%Fe-6wt%Ni-3wt.%Co cemented carbides has been investigated for different carbon contents. Low melting eutectics (1200ºC-1218ºC) are detected on first heating for Cr contents of 1 and 2 wt.% and for C contents near the upper bound of the corresponding C windows. These eutectics disappear on repeated heating and cooling experiments, being substituted by narrower peaks occurring at higher temperatures. These phenomena are likely related to the decarburization associated to carbothermal reduction of powder oxides and the homogeneization of the chemical composition of these multicomponent binder phases. Thermocalc® predictions of melting and solidification temperature ranges are closer to experimental data for high Cr contents. The predicted location of C windows, defined in this work by the absence of free C or $\eta$ phases, is displaced to lower C contents when compared with experimental results. As expected from their high Ni content, binder phases are mainly austenitic for high C compositions. However, a BCC phase is partially stabilized in compositions with low C and high Cr contents. In compositions with neither free C nor $\eta$ phases, high magnification SEM images show the presence of submicron Cr-rich carbides precipitated at the WC-metal interface. These Cr-rich carbides disappear in composition C4 with 0.75 wt.% Cr and 5.39 wt.% C. This C content is 0.17 wt.% higher than that predicted by Thermocalc ®.for precipitation of $M_7C_3$.

## Acknowledgments

Fabricación de Metales Duros S.A.L. FMD CARBIDE, L&L ROTARY SOLUTIONS and CDTI (Centro para el Desarrollo Tecnológico Industrial) are gratefully acknowledged by the financial support of this work. T. Soria-Biurrun gratefully acknowledges the Department of Education of Navarra Government for the finantial support of his doctoral thesis.

## References

1- REACH, http://ec.europa.eu/environment/chemicals/reach/reach_intro.htm.

2- Wild P, Perdrix A, Romazini S, Moulin JJ, Lung cancer mortality in a site producing hard metals, Occup. Environ. Med. 57 (2000) 568–73.

3- Leyssens L, Vinck B, Van Der Straeten C, Wuyts F, Maes L; Cobalt toxicity in humans—A review of the potential sources and systemic health effects, Toxicology 387 (2017) 43–56.

4- Report on Critical Raw Materials for the EU, May 2014, Report of the Ad hoc Working Group on defining critical raw materials. http://www.catalysiscluster.eu/

5- https://ec.europa.eu/jrc/sites/jrcsh/files/cobalt_infographics_one-pager.pdf

6- Roebuck B, Almond EA, A comparison of the deformation characteristics of Co and Ni alloys containing small amounts of W and C, Proceed. 10th Plansee Serninar, Metallwerk Plansee, Reutte, Austria, Vol. 1, (1981), 493-508.

7- Ekemar S, Lindholm L, Hartzell T, Nickel as a binder metall in WC-based cemented carbides. Int. J. Refract. Met. Hard Mater., March, (1982), 37-40.

8- Prakash L, Development of tungsten carbide hardmetals using iron based binder alloys. [PhD Thesis] Germany: University of Karlsruhe; 1979.

9- Schubert WD, Fugger M, Wittmann B, Useldinger R, Aspects of sintering of cemented carbides with Fe-based bindersInt. J. Refract. Met. Hard Mater. 49 (2015) 110-23.

10- García J, Cemented carbide microstructures: a review, Int. J. Refract. Met. Hard Mater., 80 (2019) 40-68.

11- Zhang F, Zhang C, Chen SL, Zhu J, Cao WS, Kattner UR, An understanding of high entropy alloys from phase diagram calculations, Calphad 45 (2014) 1–10.

12- Toller L, Liu CX, Holmström E, Larsson T, Norgren S, Investigation of cemented carbides with alternative binders afterCVD coating Int. J. Refract. Met. Hard Mater. 62 (2017) 225–29.

13- Linder D, Holmström E, Norgren S, High entropy alloy binders in gradient sintered hardmetal, Int. J. Refract. Met. Hard Mater. 71 (2018) 217–20.

14- Holmström E, Lizárraga R, Linder D, Salmasi A, Wang W, Kaplan B, Mao H, Larsson H, Vitos L, High entropy alloys: substituting for cobalt in cutting edge technology, Appl. Mater. Today 12 (2018) 322–29.

15- Frisk K, Markström A, Effect of Cr and V on phase equilibria in Co–WC based hardmetals,‖ Int. J. Mater. Res., 99, 3, (2008), 287–93.

16- de Oro Calderon R, Edtmaier C, Schubert WD, Novel binders for WC-based cemented carbides with high Cr contents. Int. J. Refract. Met. Hard Mater. 85 (2019) 105063.

17- Tarraste M, Kübarsepp J, Juhani K, Mere A, Kolnes M, Viljus M, Maaten B, Ferritic chromium steel as binder metal for WC cemented carbides, Int. J. Refract. Met. Hard Mater. 73 (2018) 183–91.

18- de Oro Calderon R, Agna A, Gomes UU, Schubert WD, Phase formation in cemented carbides prepared from WC and stainless steel powder – An experimental study combined with thermodynamic calculations Int. J. Refract. Met. Hard Mater. 80 (2019) 225–37.

19- Chen CS, Yang CC, Chai HY, Yeh JW, Chau JLH, Novel cermet material of WC/multielement alloy, Int. J. Refrac. Metals Hard Mater. 43 (2014) 200–04.

20- de la Obra AG, Avilés MA, Torres Y, Chicardi E, Gotor FJ, A new family of cermets: Chemically complex but microstructurally simple, Int. J. Refract. Met. Hard Mater. 63 (2017) 17–25.

21- SETARAM Instrumentation. Setsys evolution 16/18. SETSOFT user manual, (2002), 39.

22- Haglund S, Ågren J, Uhrenius B. Solid state sintering of cemented carbides—an experimental study. Z Metallkd 1998;89:316–22.

23- Petersson A, Sintering shrinkage of WC–Co and WC–(Ti,W)C–Co materials with different carbon contents Int. J. Refract. Met. Hard Mater., 22, (2004), 211-217.

24- Frisk K, Markström A, Effect of Cr and V on phase equilibria in Co–WC based hardmetals, Int. J. Mater. Res, 99, 03, (2008), 287-93.

25- Cullity BD, Elements of X-Ray Diffraction, Addison-Wesley Publish. Co., Inc., 1956, 391-93.

26- Roulon Z, Missiaen JM, Lay S, Carbide grain growth in cemented carbides sintered with alternative binders, Int. J. Refract. Met. Hard Mater. 86 (2020) 105088

**FIGURE CAPTIONS**

**Fig. 1** (a) Shrinkage vs. temperature of compositions C1 and C2 in Table 1. Both are WC-15wt.% (40Fe40Ni20Co) alloys with high and low C contents respectively within the C window, (b) shrinkage rate vs. temperature of the same compositions, (c) DSC plots corresponding to the same thermal cycle.

**Fig. 2** Isopleth corresponding to W-C-Fe-Ni-Co system calculated with Thermocalc® software using TCFE10 database.

**Fig. 3** BSE-SEM micrograph of the surface of a green compact corresponding to composition C4_medium C content (see Table 2).

**Fig. 4** Effect of three repeated thermal cycles on DSC heat flow vs. temperature curves: (a) alloy C1 and (b) Alloy C2.

**Fig. 5** Shrinkage and shrinkage rate of WC-FeNiCo (40/40/20) alloys with different Cr additions: (a and b) compositions with high C content, (c and d) compositions with low C content.

**Fig. 6** DSC plots corresponding to WC-FeNiCoCr alloys with high C contents: (a) Alloy C3 (0.74wt.%Cr), (b) Alloy C6 (1wt.%Cr) and (c) Alloy C8 (2wt.%Cr). Data from 1$^{st}$ and 3$^{rd}$ repeated thermal cycle are included in all cases.

**Fig. 7** Id. as Fig. 4 for WC-FeNiCoCr alloys with low C contents: (a) Alloy C5 (0.74wt.%Cr), (b) Alloy C7 (1wt.%Cr) and (c) Alloy C9 (2wt.%Cr). Data from 1$^{st}$ and 3$^{rd}$ repeated thermal cycle are included in all cases.

**Fig. 8** Isopleths corresponding to W-C-Fe-Ni-Co-Cr systems with increasing Cr contents calculated with Thermocalc® software: (a) 0.75 wt.%Cr, (b) 1 wt.%Cr and (c) 2 wt.%Cr. TCFE10 database.

**Fig. 9** Temperatures corresponding to the onset and end of solidification peaks detected in the 1st and 3rd DSC cycles: (a) High C alloys and (b) Low C alloys. Blue rectangles represent the solidification ranges estimated by Thermocalc ® (TCFE10).

**Fig. 10** X-ray diffraction patterns corresponding to high and low C WC-FeNiCo alloys with different Cr additions: (a) 0 wt.%, (b) 0.75 wt.%, (c) 1 wt.% and (d) 2 wt.%.

**Fig. 11** Estimation of FCC vol. fraction in the binder phase of WC-FeNiCoCr alloys by the direct comparison method [25].

**Fig. 12** BSE-SEM micrographs corresponding to WC-FeNiCoCr alloys. Compositions C1,C4, C6 and C8 correspond to high C contents and C2, C5, C7 and C9 to low C ones.

**Fig. 13** BSE-SEM high magnification image of composition C8 along with EDS mappings of main constitutive elements. Red arrows identify Cr-rich carbides which precipitate at the WC-metal interface. Cr content (12 wt.%) is calculated with respect to Fe+Ni+Co+Cr nominal content of the alloy.

**Fig. 14** BSE-SEM high magnification images corresponding to: (a) alloy C3 (high C) and (b) alloy C5 (low C). EDS mappings of alloy C5 (c) show no precipitation of Cr-rich phases.

Figure 2

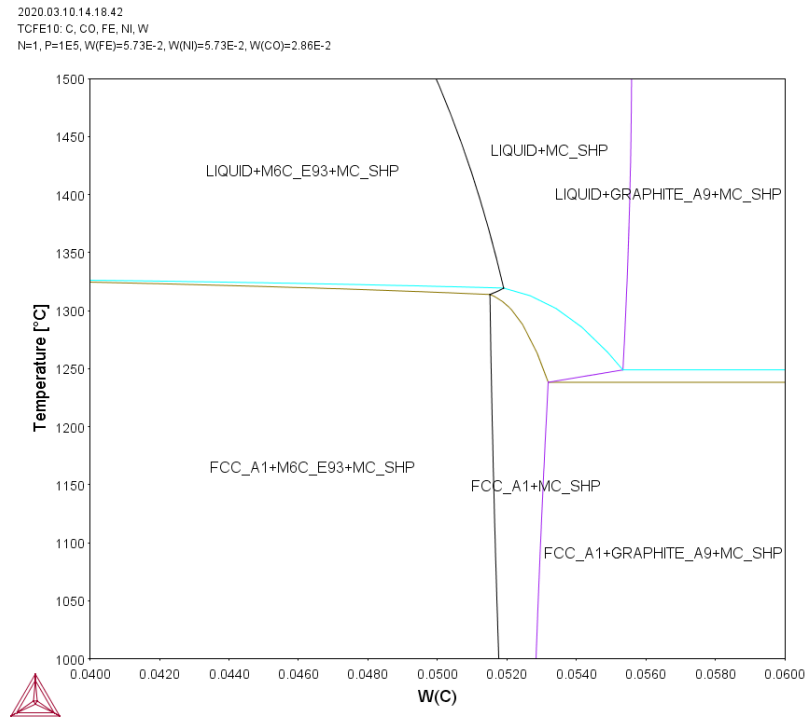


Fig. 2

Figure 3

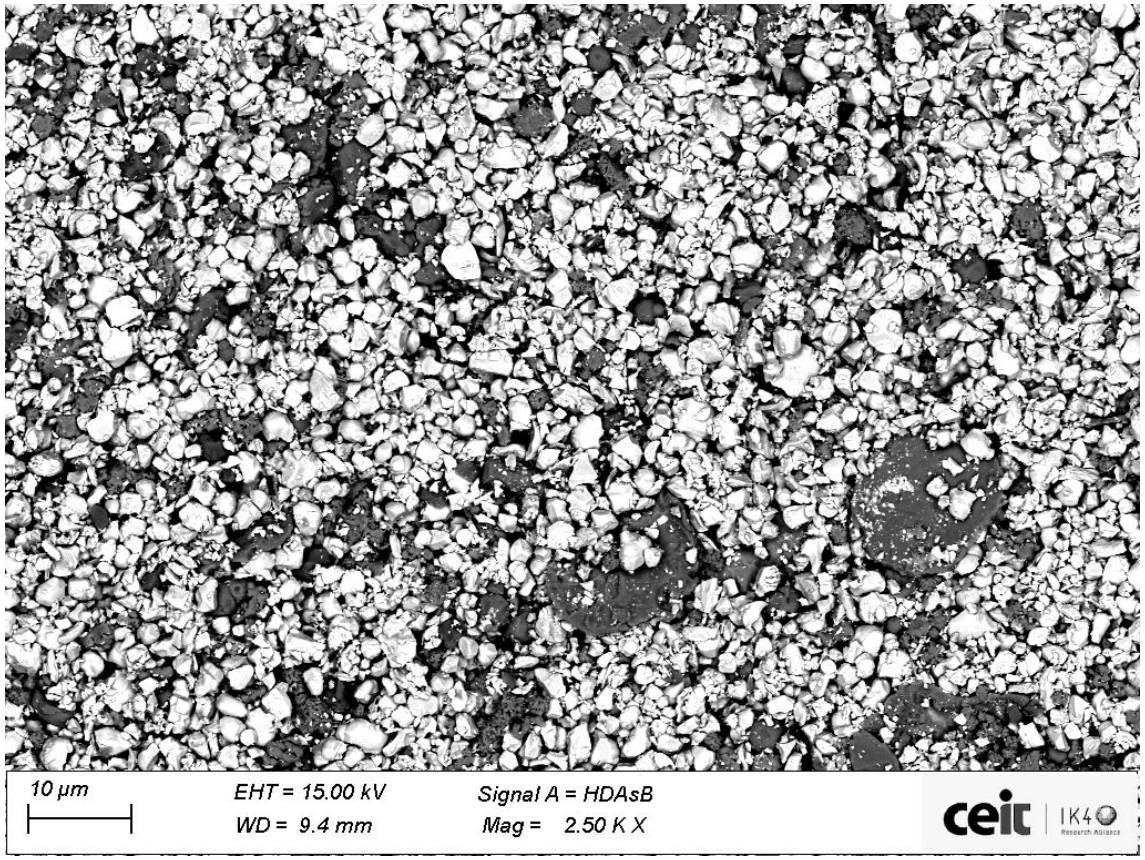


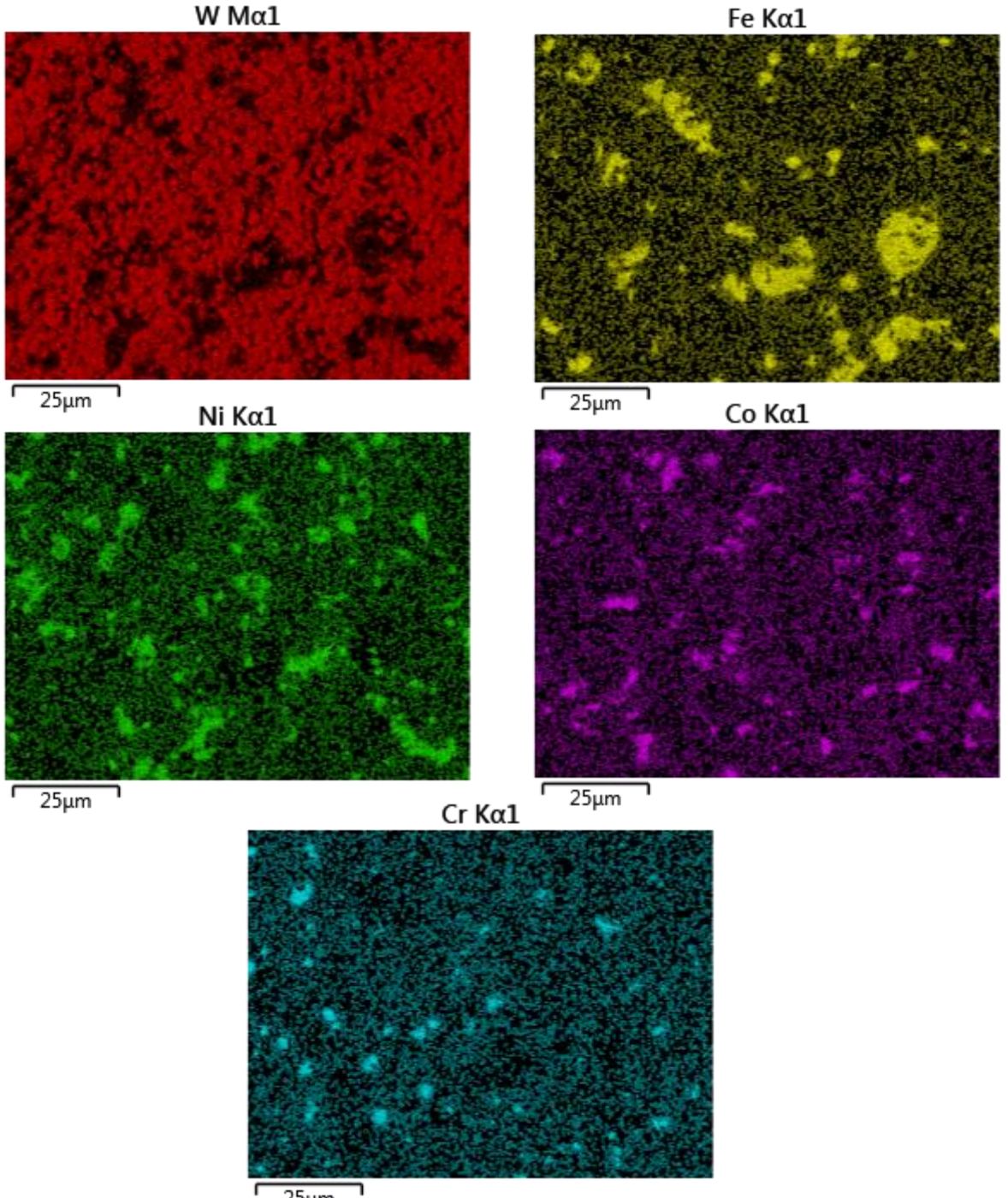


Fig. 3

Figure 4

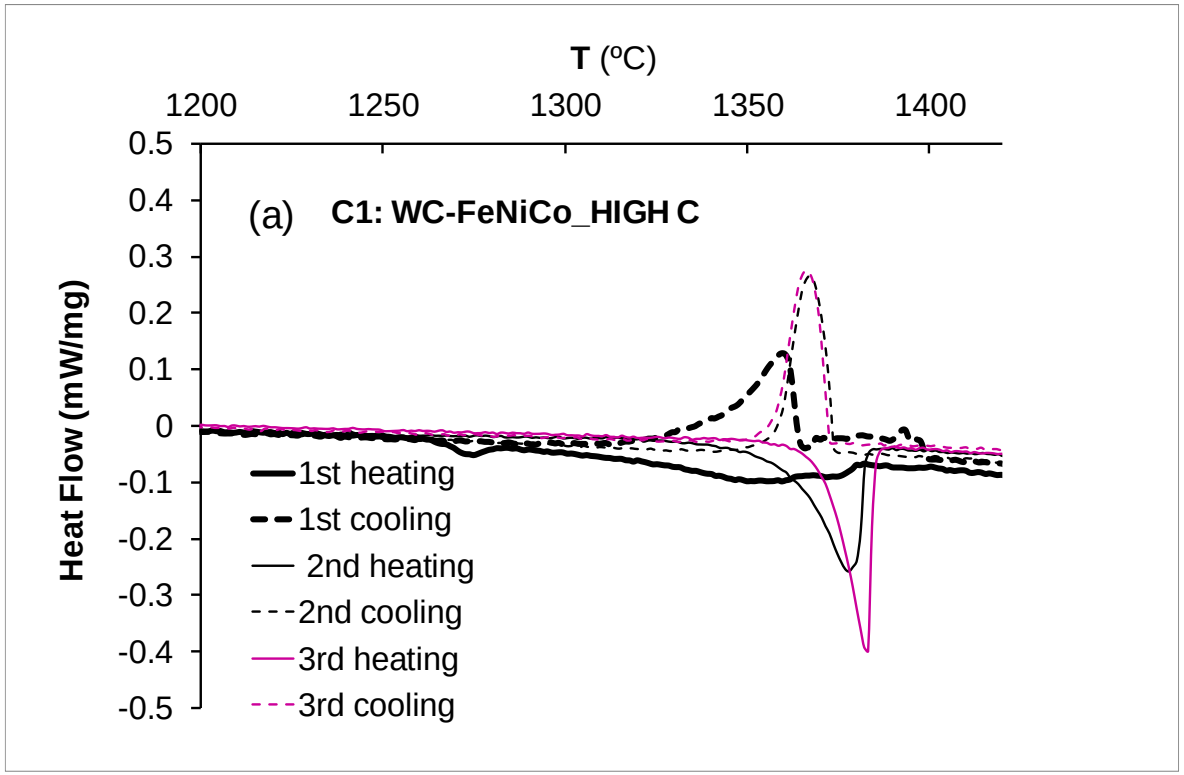


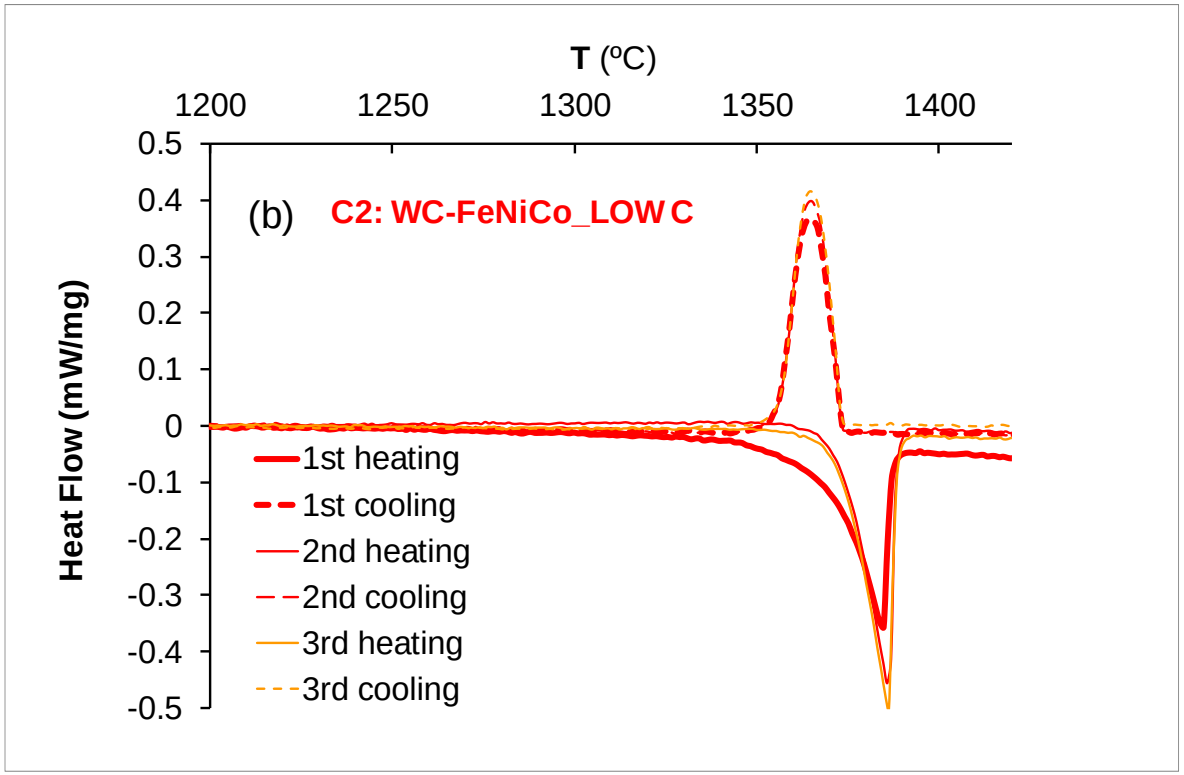


Fig. 4

Figure 5

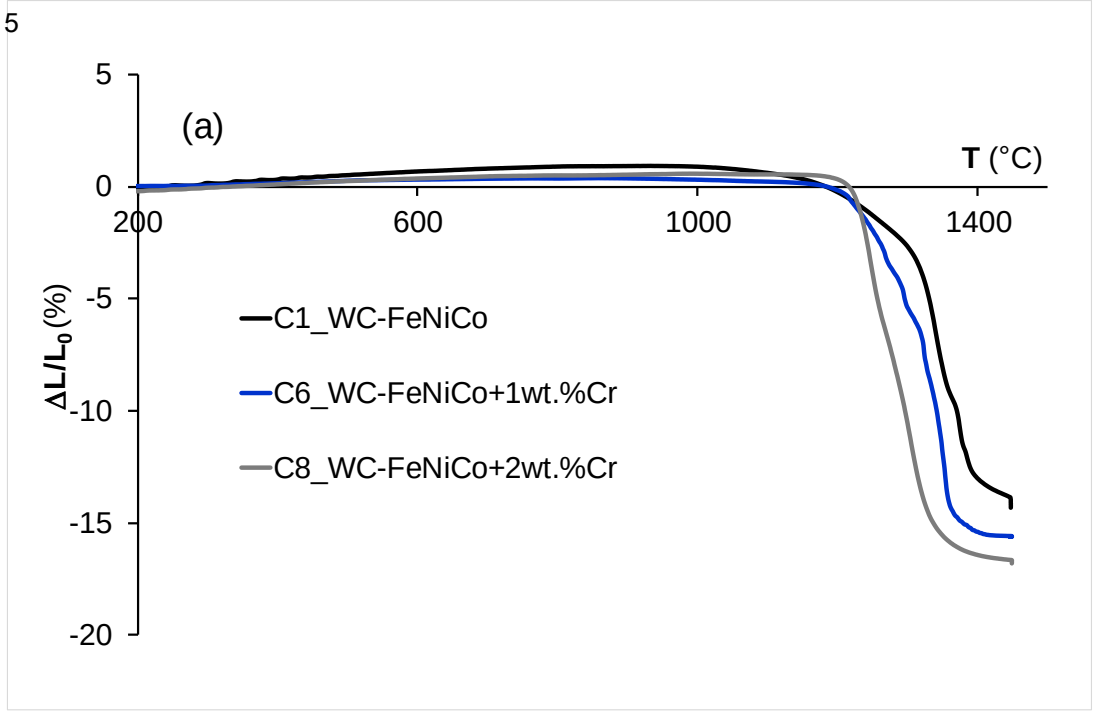


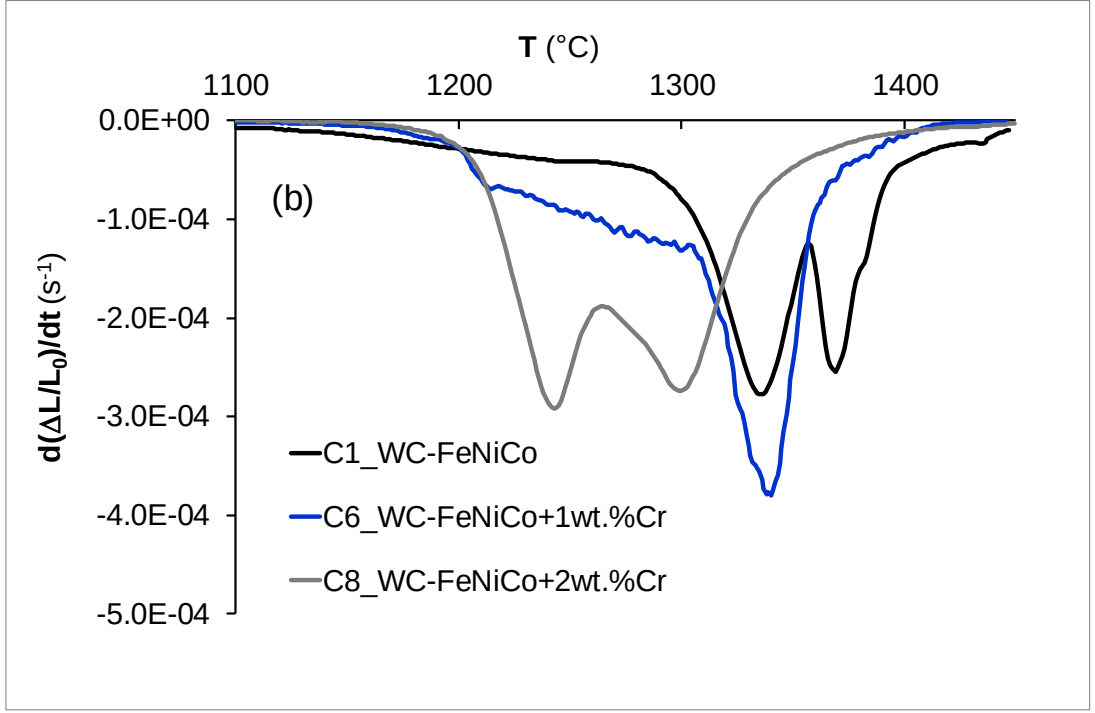


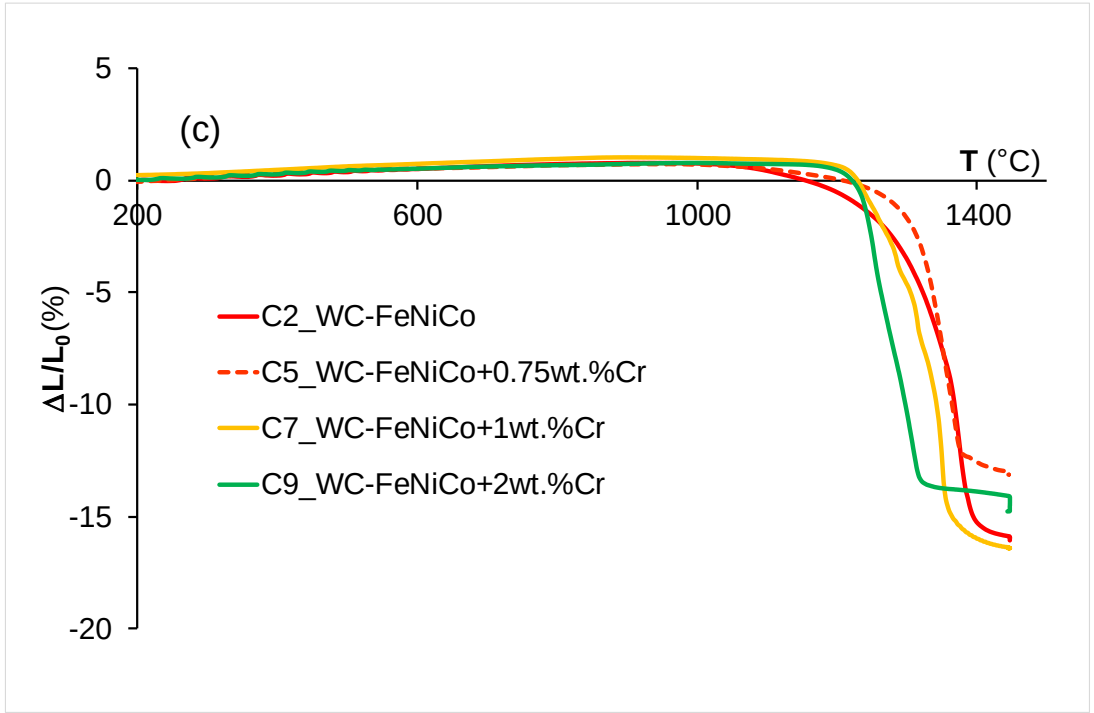


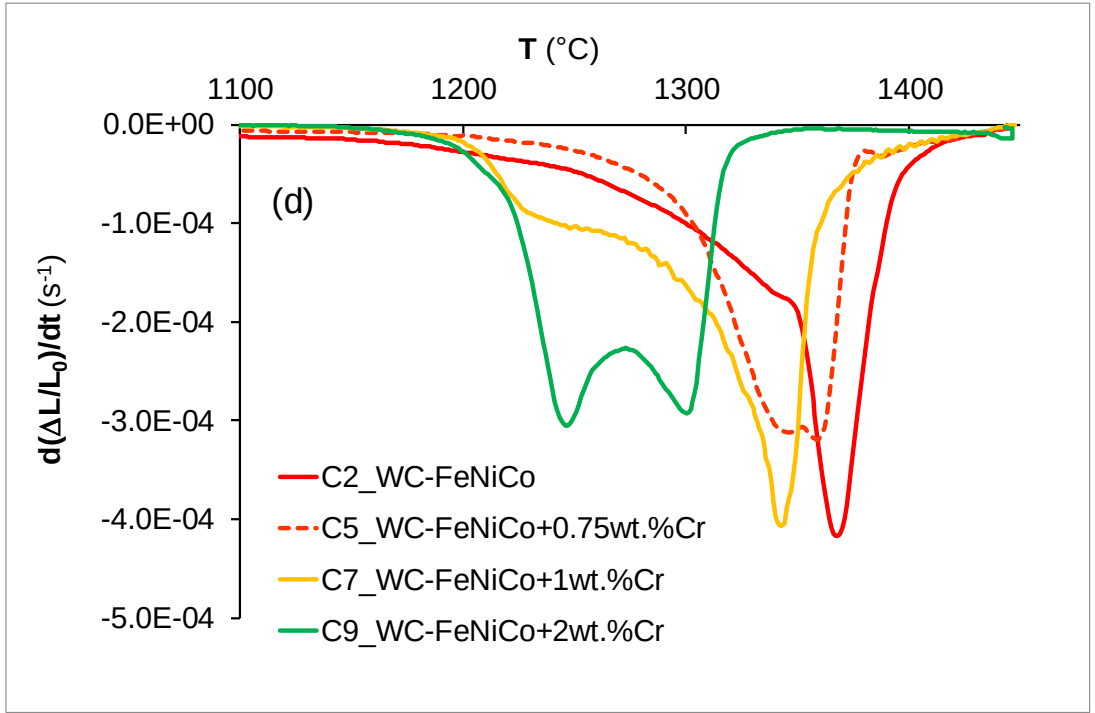


Fig. 5

Figure 6

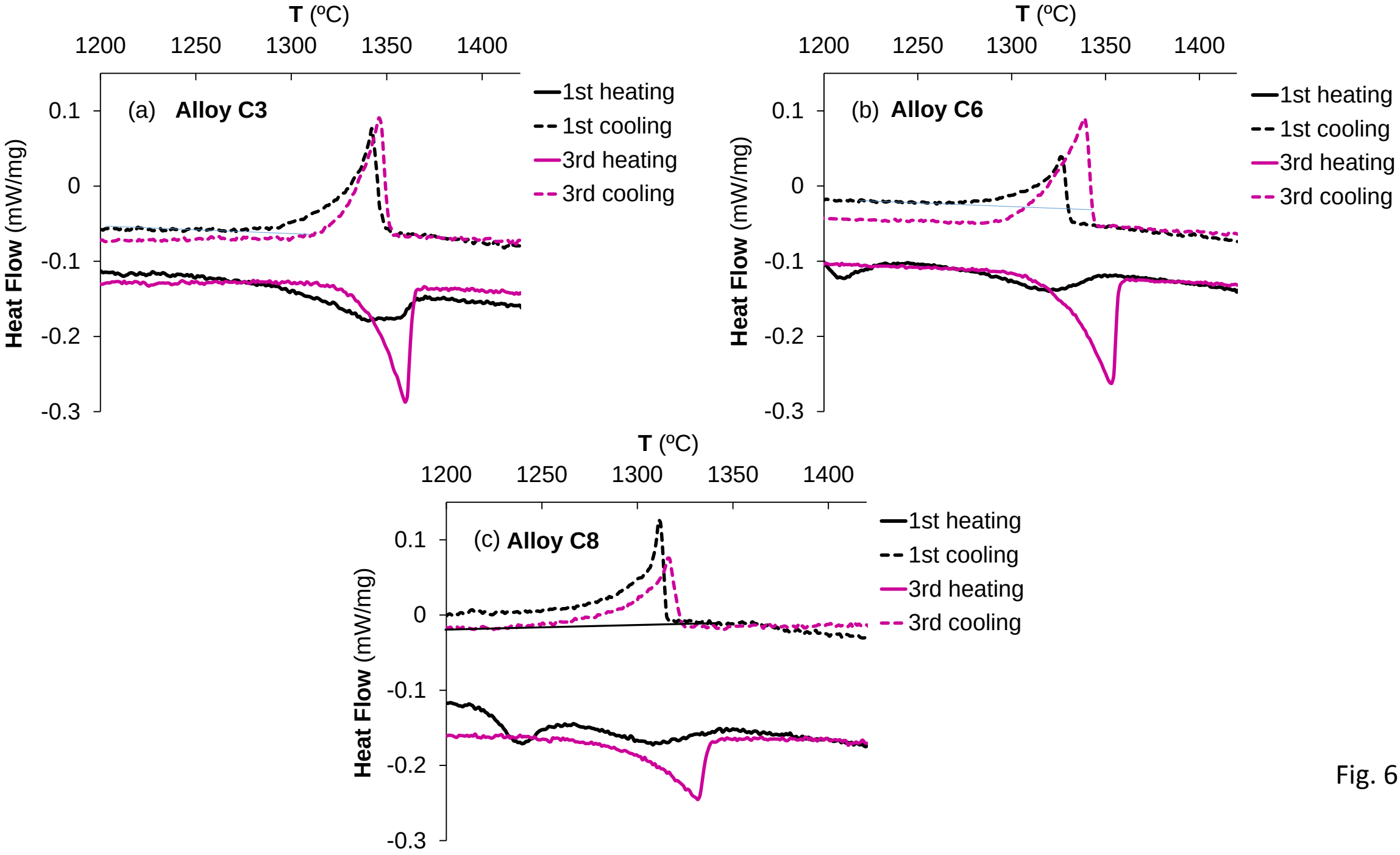


Fig. 6

Figure 7

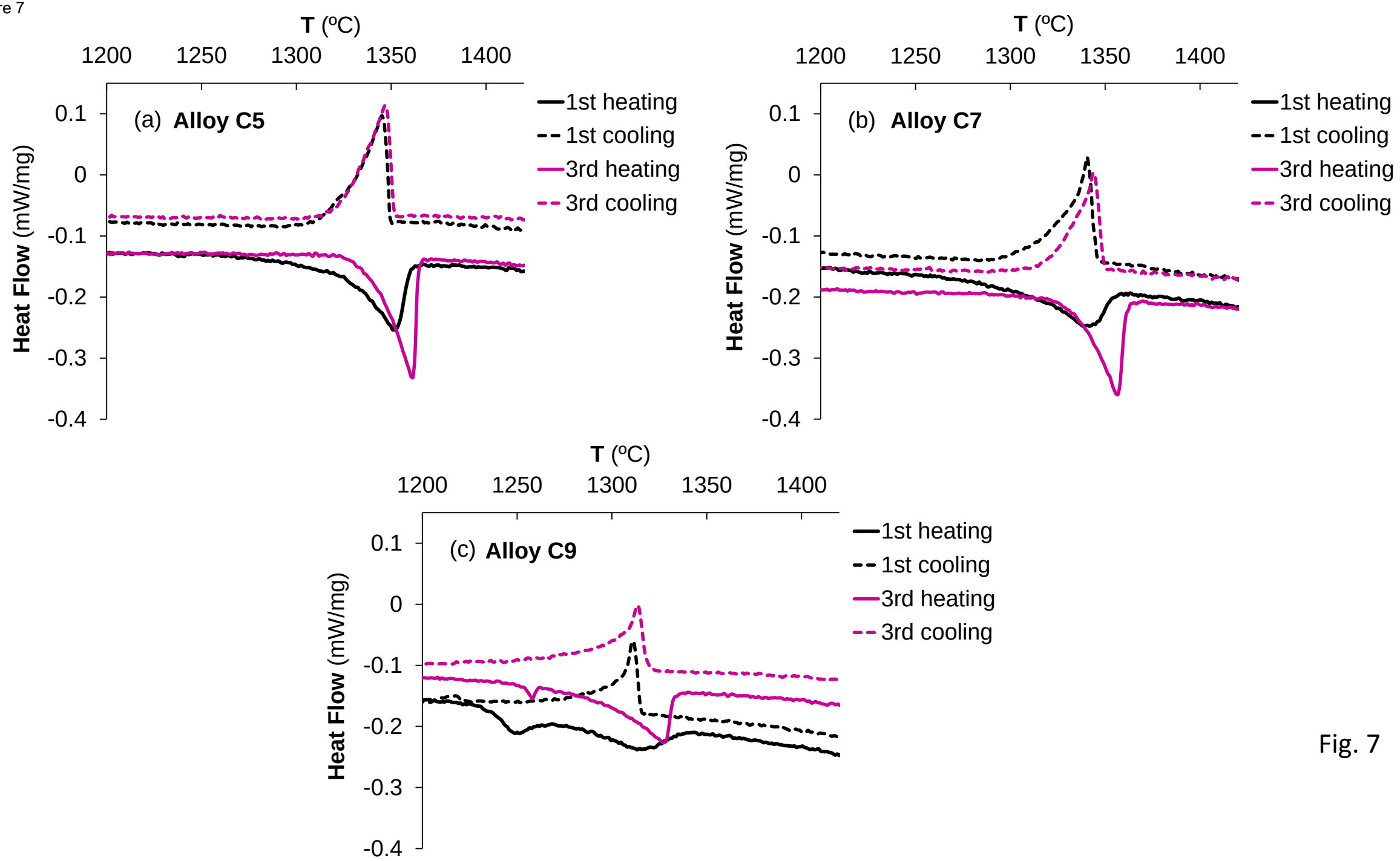


Fig. 7

Figure 8

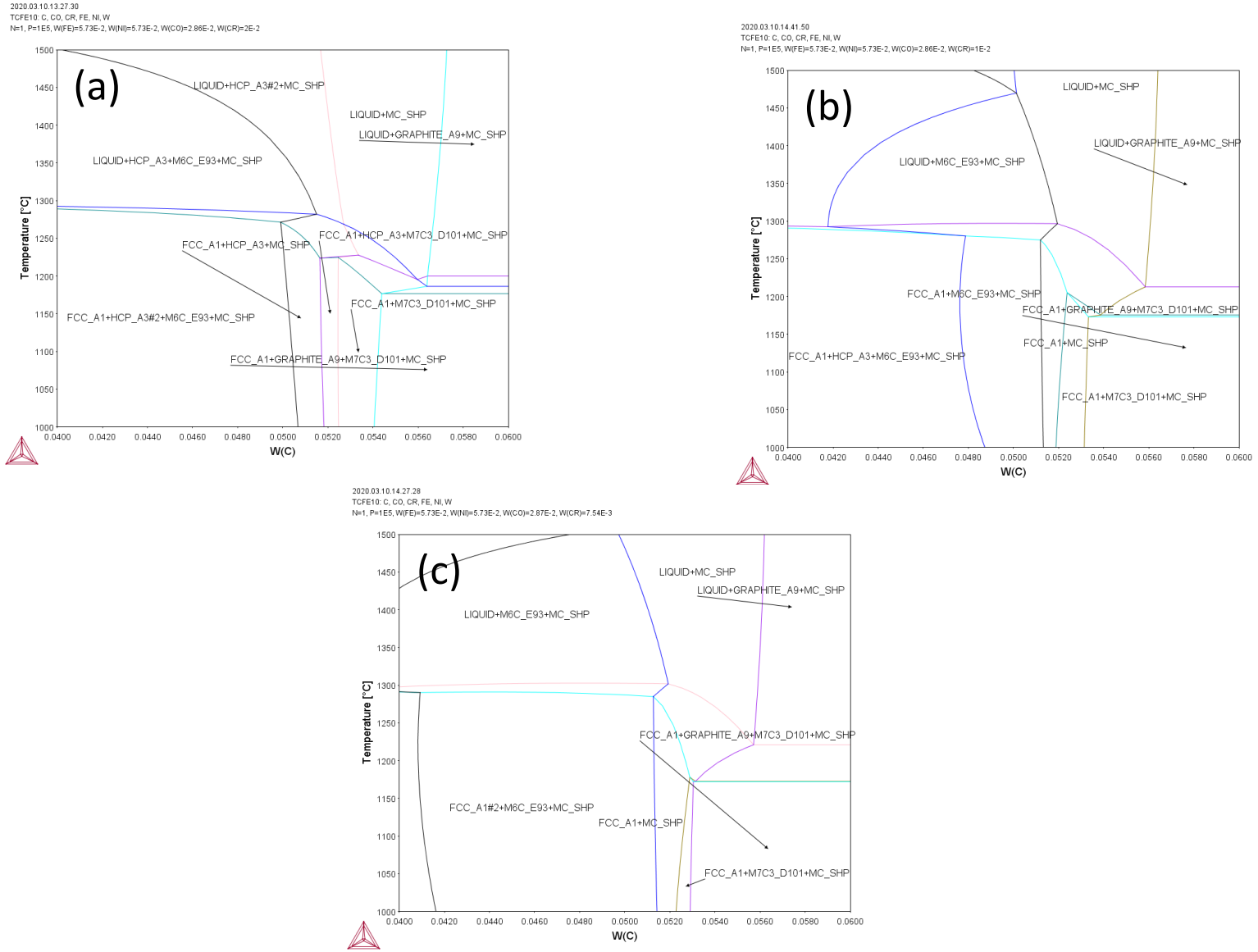


Fig. 8

Figure 9

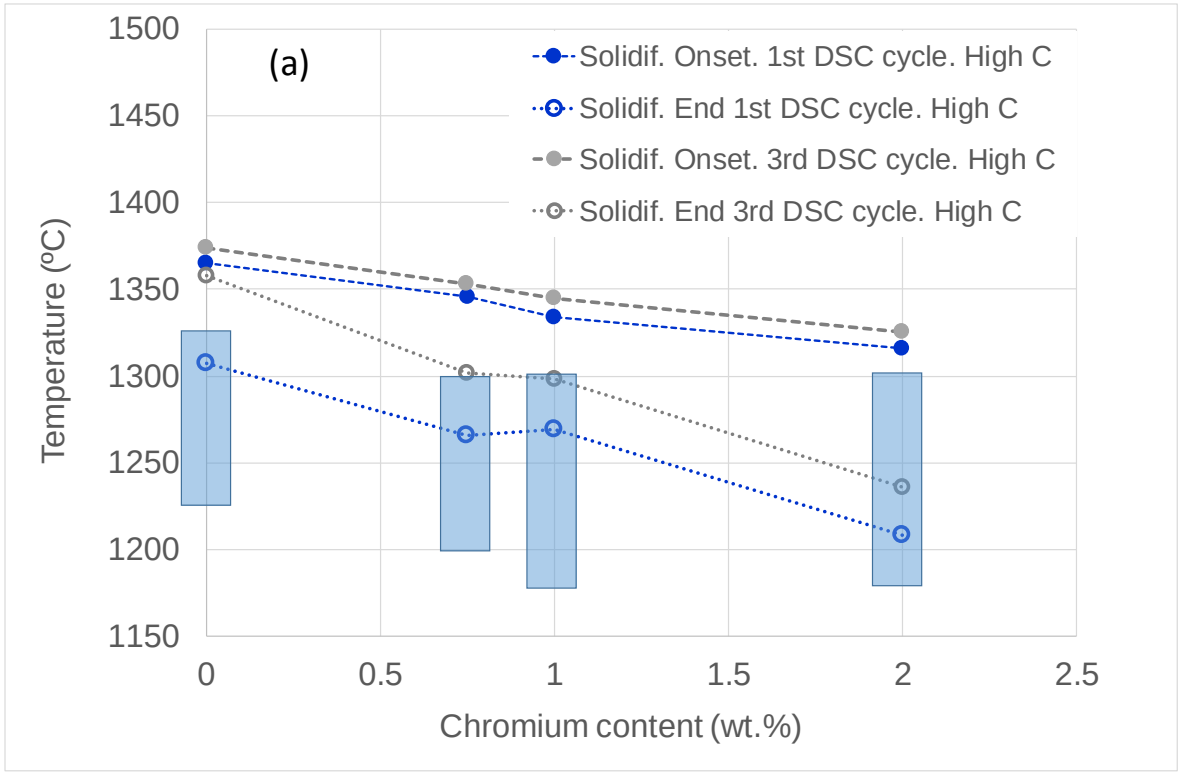


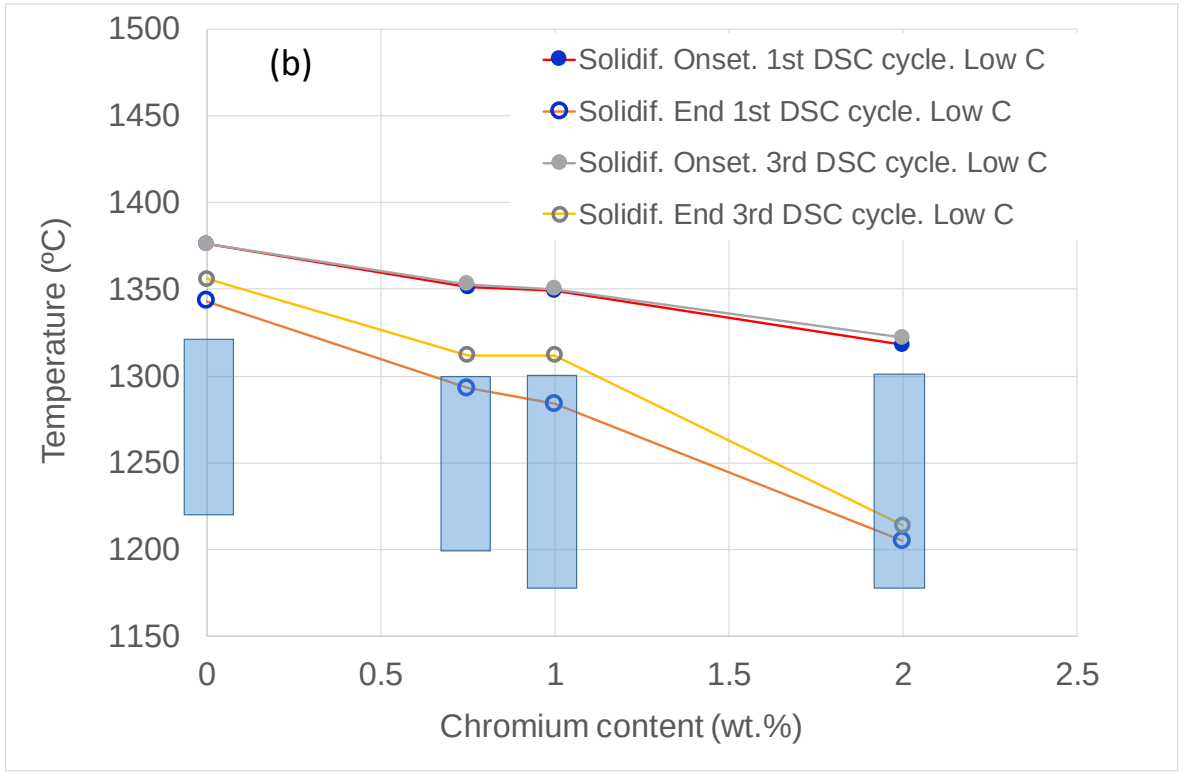


Fig. 9

Figure 10

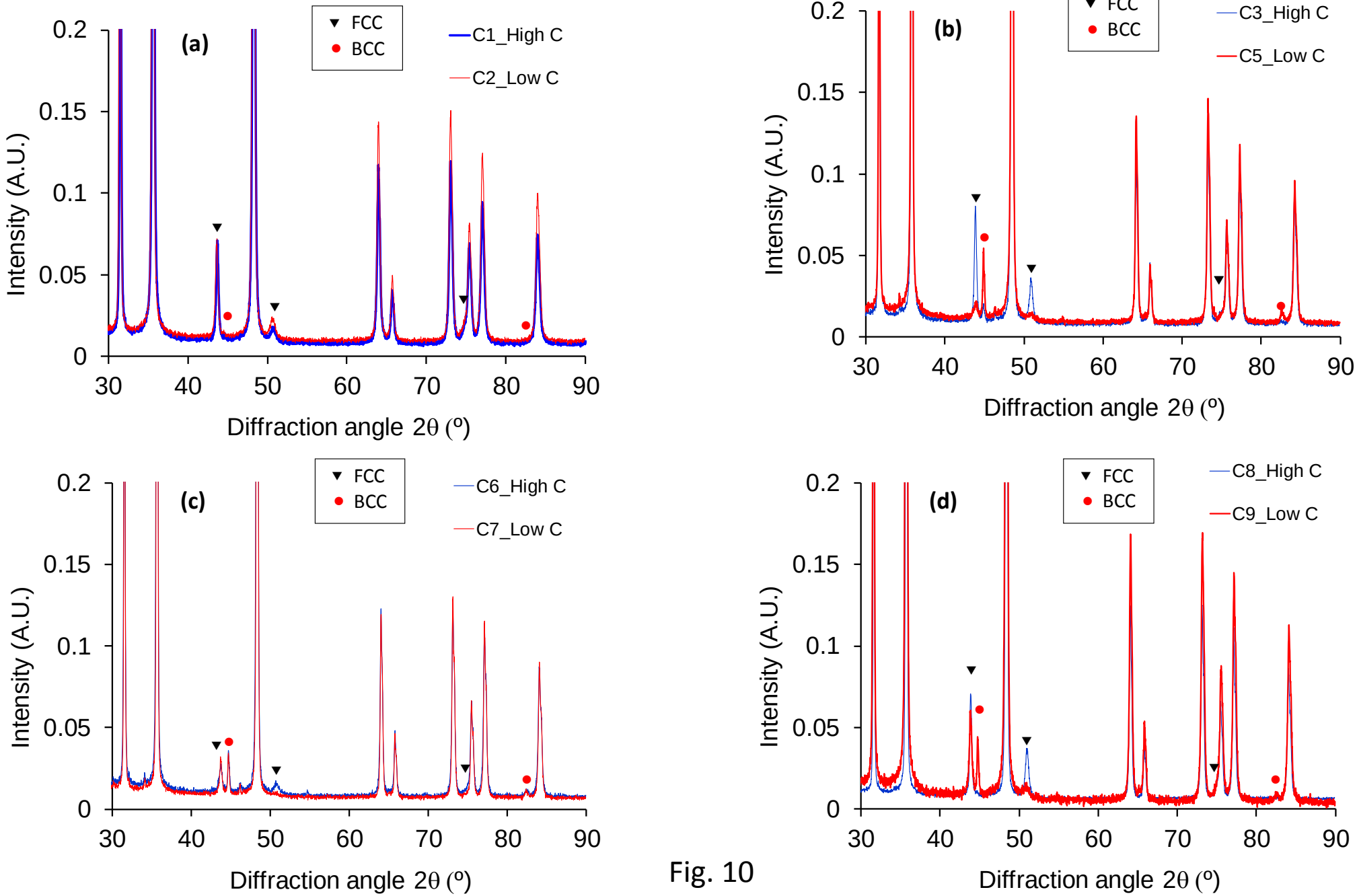


Fig. 10

Figure 11

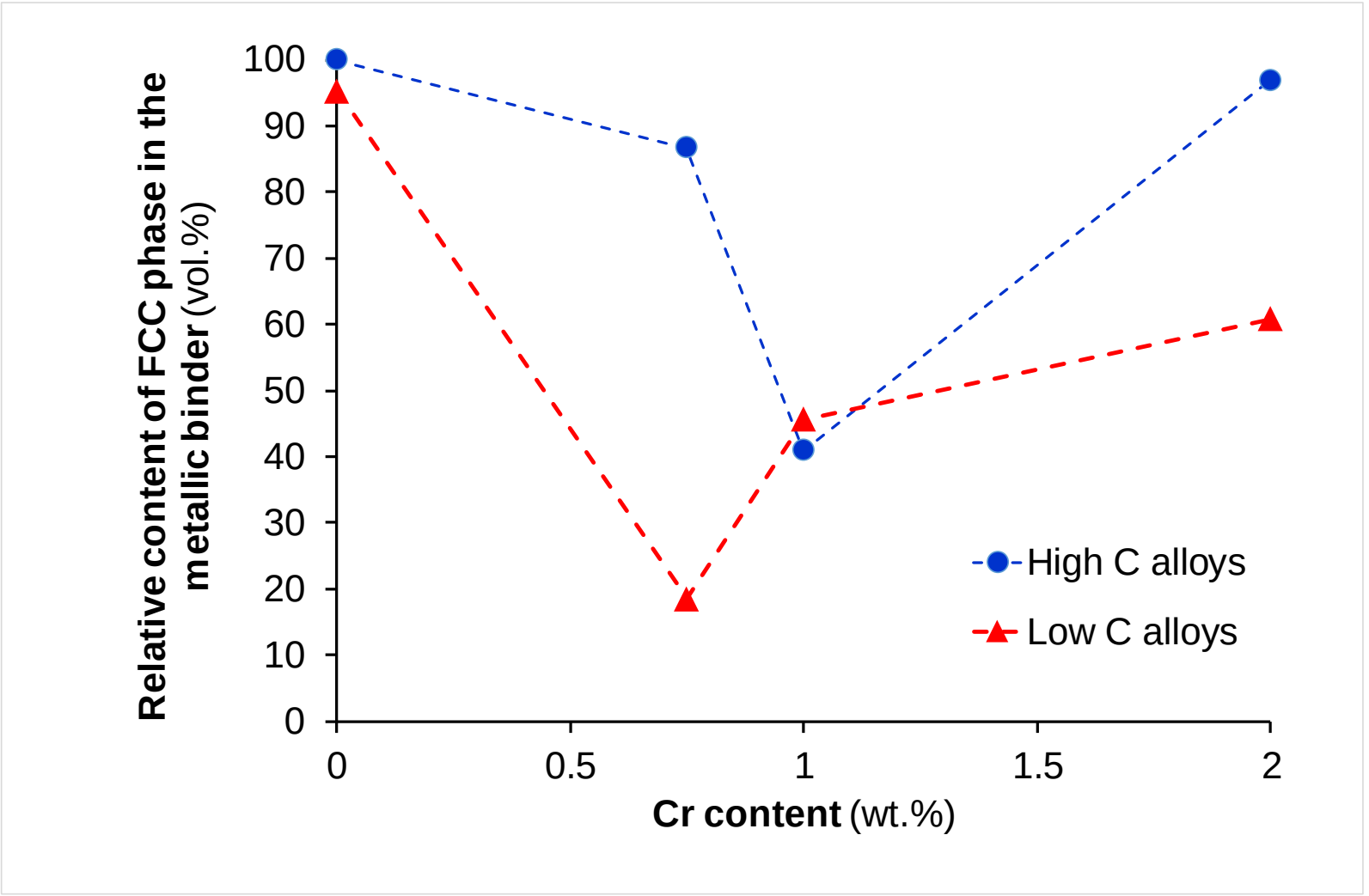


Fig. 11

Figure 12

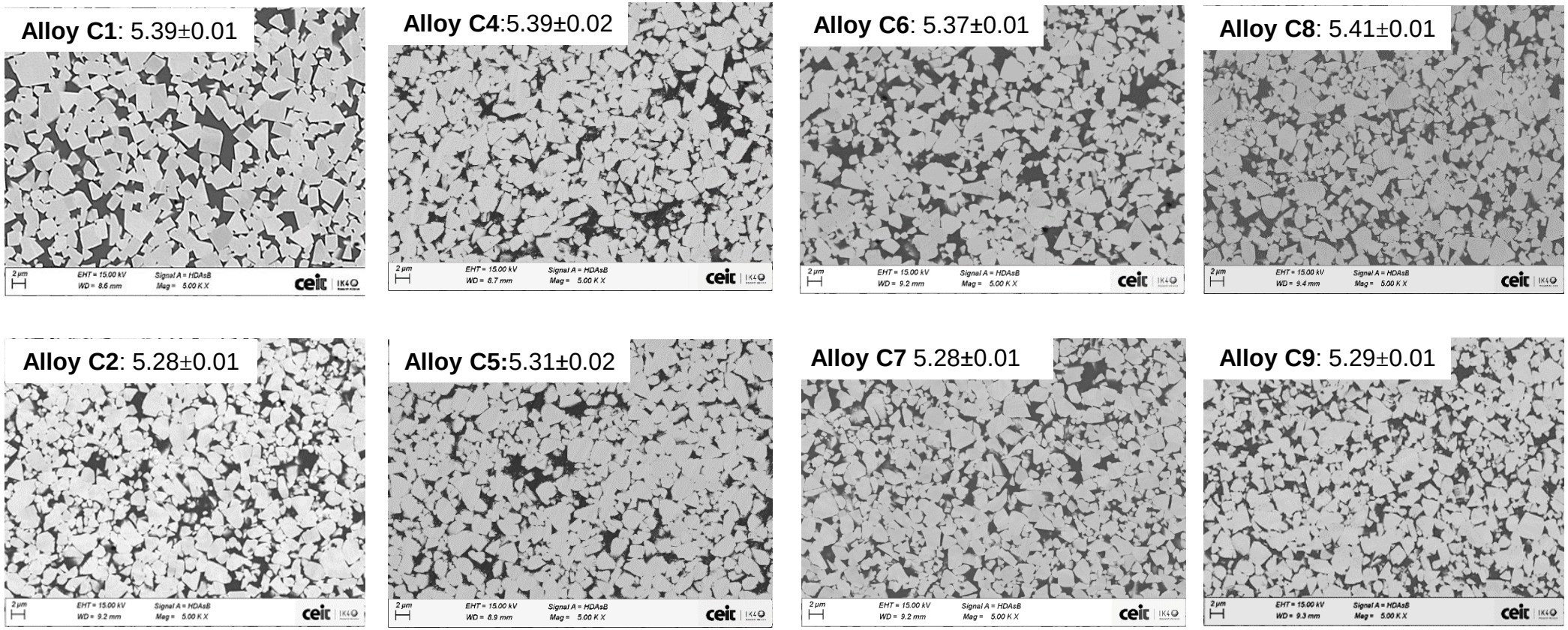


Fig. 12

Figure 13


**Alloy C8**
**WC-FeNiCoCr (wt.%)**
**(35.2/35.2/17.5/12)**

Fig. 13

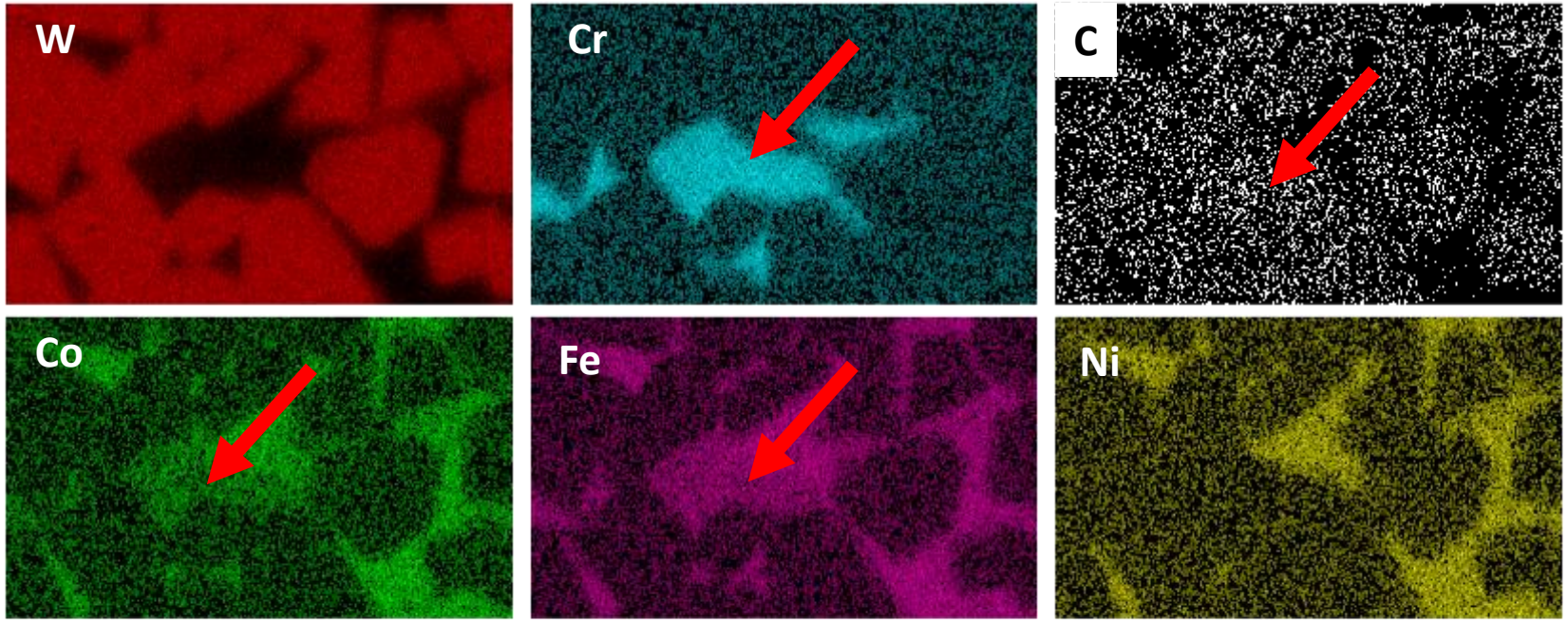

Figure 14

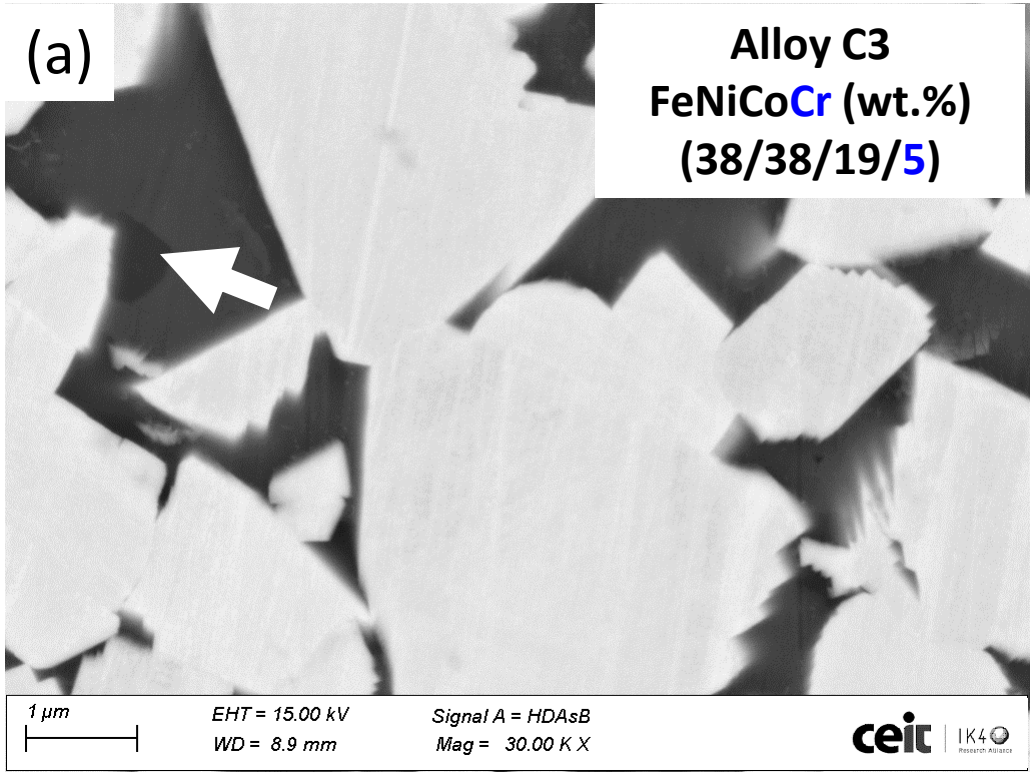


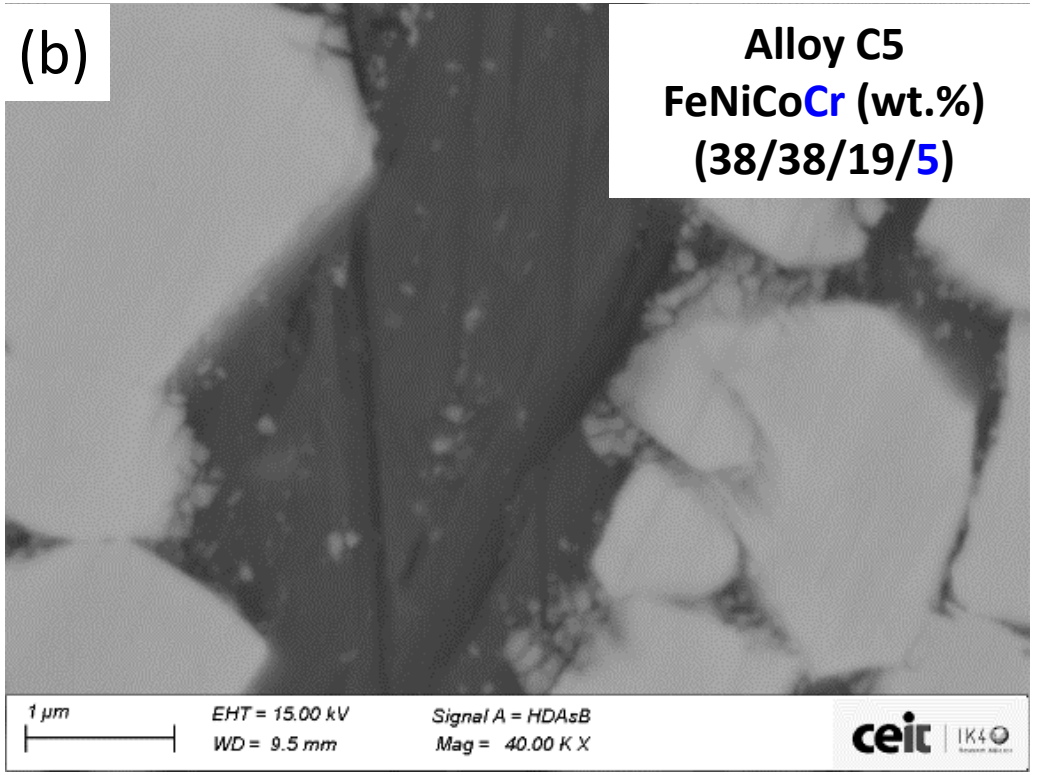


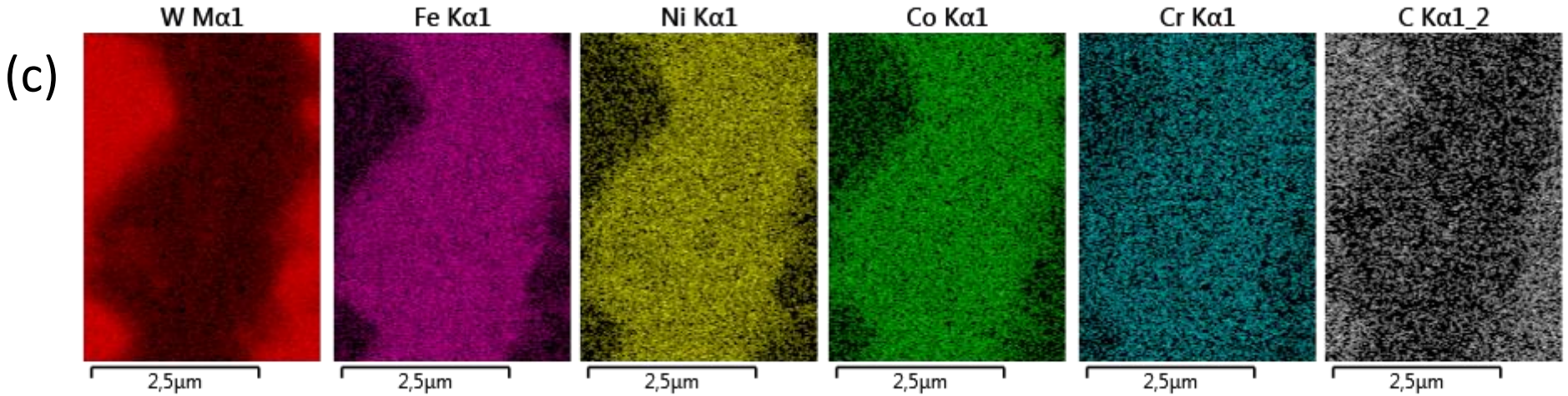


Fig. 14

Table 1

Click here to access/download

**Table**

Table 1.docx

Table 2

Click here to access/download

**Table**

Table 2.docx

Table 3

Click here to access/download

**Table**

Table 3.docx

Table 4

**Declaration of interests**

☒ The authors declare that they have no known competing financial interests or personal relationships that could have appeared to influence the work reported in this paper.

☐The authors declare the following financial interests/personal relationships which may be considered as potential competing interests:

Corresponding autor on behalf of all coauthors

Jose M. Sanchez Moreno

Dear Editor,

We the undersigned declare that this manuscript entitled "Effect of Cr anc C contents on the sintering of WC-Fe-Ni-Co-Cr multicomponent alloys" is original, has not been published before and is not currently being considered for publication elsewhere.

We confirm that the manuscript has been read and approved by all named authors and that there are no other persons who satisfied the criteria for authorship but are not listed. We further confirm that the order of authors listed in the manuscript has been approved by all of us.

We understand that the Corresponding Author is the sole contact for the Editorial process. He is responsible for communicating with the other authors about progress, submission of revisions and final approval of proofs.

On behalf of the corresponding author

Jose M. Sanchez Moreno